AN ABSTRACT OF THE DISSERTATION OF

Michael A. Starrett for the degree of Doctor of Philosophy in Electrical and Computer Engineering presented on May 31, 2016.

Title: Development and Experimental Hardware Validation of Novel Variable Speed Hydropower Control Schemes for Emerging Applications and Water Resource Paradigms

Abstract approved:

_____

Ted K.A. Brekken

Recent opportunities for new hydropower generation in the United States have often been in non-powered dams and run-of-river type flows occurring in low-impact natural areas and unregulated conduits. At the same time, a changing water resource paradigm is challenging some existing generation in drought stricken areas where supply reservoirs behind many medium and high head units are at historically low levels. The result is a developing market space which is potentially best captured by machines capable of variable speed operation. Variable speed units have a wider range of operating conditions compared to their synchronous counterparts and have already proven their resilience through a 20+ year history in pumped hydro applications. This work develops a control scheme for variable speed hydropower units operating to deliver a set-point power through flow controlling gates. This control scheme increases both the hydrologic operating range of a unit as well as the speed of response to grid contingencies under droop and automatic generator control. Results from simulation are confirmed on hardware.

Development and Experimental Hardware Validation of Novel Variable Speed Hydropower Control Schemes for Emerging Applications and Water Resource Paradigms

by
Michael A. Starrett

A DISSERTATION

submitted to

Oregon State University

in partial fulfillment of
the requirements for the
degree of

Doctor of Philosophy

Presented May 31, 2016
Commencement June 2016

Doctor of Philosophy dissertation of Michael A. Starrett presented on May 31, 2016

APPROVED:

Major Professor, representing Electrical and Computer Engineering

Director of the School of Electrical Engineering and Computer Science

Dean of the Graduate School

I understand that my dissertation will become part of the permanent collection of Oregon State University libraries. My signature below authorizes release of my dissertation to any reader upon request.

Michael A. Starrett, Author

ACKNOWLEDGEMENTS

With tremendous gratitude to my adviser, Dr. Ted Brekken. Thank you for all that you taught me, the effort you put in to helping to support my graduate studies, and the patience and humility that you showed me while I was learning. Your investment in my growth is so appreciated and I am a better person for having worked under your guidance.

With honest thanks to my committee members, Dr. Annette von Jouanne, Dr. Eduardo Cotilla-Sanchez, and Dr. Julia Zhang. The Energy Systems faculty group is a tremendous asset to the student members and I benefited greatly from the expertise lent by all.

With great appreciation to all of my colleagues in the energy systems group, and with a special acknowledgement to Ziwei Ke, Lei Jin, Han Xiong, Jia Jia Song and Ratanak So. Thank you to each of you for your friendship; it was a great honor to be your peer.

And finally, with a sincere sense of indebtedness to my better half, Jess, who graciously supported me as a voice of encouragement, a careful proof-reader, a good listener, an intellectual contributor, and partner in every high and every low throughout my entire doctoral program.

Thank you to all.

TABLE OF CONTENTS

TABLE OF CONTENTS (Continued)

LIST OF FIGURES

Figure Page

LIST OF FIGURES (Continued)

LIST OF FIGURES (Continued)

LIST OF FIGURES (Continued)

LIST OF FIGURES (Continued)

LIST OF FIGURES (Continued)

DEDICATION

To my Dad, Dr. George Starrett

DEVELOPMENT AND EXPERIMENTAL HARDWARE VALIDATION OF NOVEL VARIABLE SPEED HYDROPOWER CONROL SCHEMES FOR EMERGING APPLICATIONS AND WATER RESOURCE PARADIGMS

1 Introduction

The history of hydropower in the United States is a story of reliability at an immense scale. Nearly 2,200 power stations built throughout the last 100 years combine to provide 80 GW of generating capacity – 7% of the national total - while also balancing the often competing priorities of flood risk management, irrigation, navigation, fisheries and wildlife management, and recreation [1]. The scale of these power stations can range from kilowatts to several gigawatts with the majority of capacity being carried by a relative handful of large (100-500 MW) and very large (>500 MW) projects (Figure 1.1). The long history of hydropower is such that roughly 75% of the total fleet capacity is located within power houses built 50 or more years ago, although modernization efforts in excess of $6B since 2005 have helped to refresh the generating equipment within a number of facilities [1].

Figure 1.1: The 2014 National Hydropower Map [2]. The Northwest holds the largest amount of capacity on the account of having many large scale projects (indicated as larger circles) whereas the Northeast has the most installed plants.

The system operators responsible for managing each station of the fleet have an excellent track record of successfully balancing complex water use priorities and are now also responding to new factors affecting the day-to-day operation and long-term future of hydropower in the United States. Broadly speaking, the new drivers for change affecting the hydropower system and overall industry are:

1. Emerging applications and federal initiatives to increase hydroelectric power production
2. Changing water resource paradigms
3. Strong growth of variable, non-dispatchable generators and the regional demand and market changes which accompany this development

Sections to follow will examine each of these drivers in detail however it is valuable to first consider the magnitude of the overall system under change. For perspective, consider the character of the hydroelectric power system along the Columbia River Basin in the Pacific Northwest:

- Drains 219,000 square miles in the U.S. to create ~45% of the nation's hydropower capacity across 133 hydroelectric dams [3].
- Irrigates 7.8 million acres of Northwest farmland by diverting 6% of the average yearly run off [4].
- A total of 56 of the 133 total dams in the Basin were developed primarily for hydroelectric generation and the remainder generate electric power as part of a multiuse projects [5].
- Includes 31 dams which are operated by federal agencies as part of a Federal Columbia River Power System (FCRPS) [6]. The FCRPS brings together three government organizations (Bonneville Power Administration (BPA), The US Army Corps of Engineers, and The Bureau of Reclamation) to manage the overall

system. BPA markets the power from these federal dams (Figure 1.2) to local and regional load centers.

- Currently, 10 of the 31 FCRPS dams are equipped with automatic generator control (AGC) and play a key role in stabilizing the power system and enabling renewable generation [7].

Figure 1.2: The 60 major dams within the Columbia River Basin [8]. BPA markets power from the 31 federals dams located throughout this region.

This resource has historically provided very inexpensive energy to utilities within the region and has been an important enabler for the 4.8 GW of wind energy developed in the BPA balancing authority area over the last 15 years (Figure 1.3). Hydropower has also been an important source of clean energy for California following the construction of two high voltage interties meant to help supply constrained utilities in the Basin export excess power to California load centers which are not predominately served by hydroelectric resources.

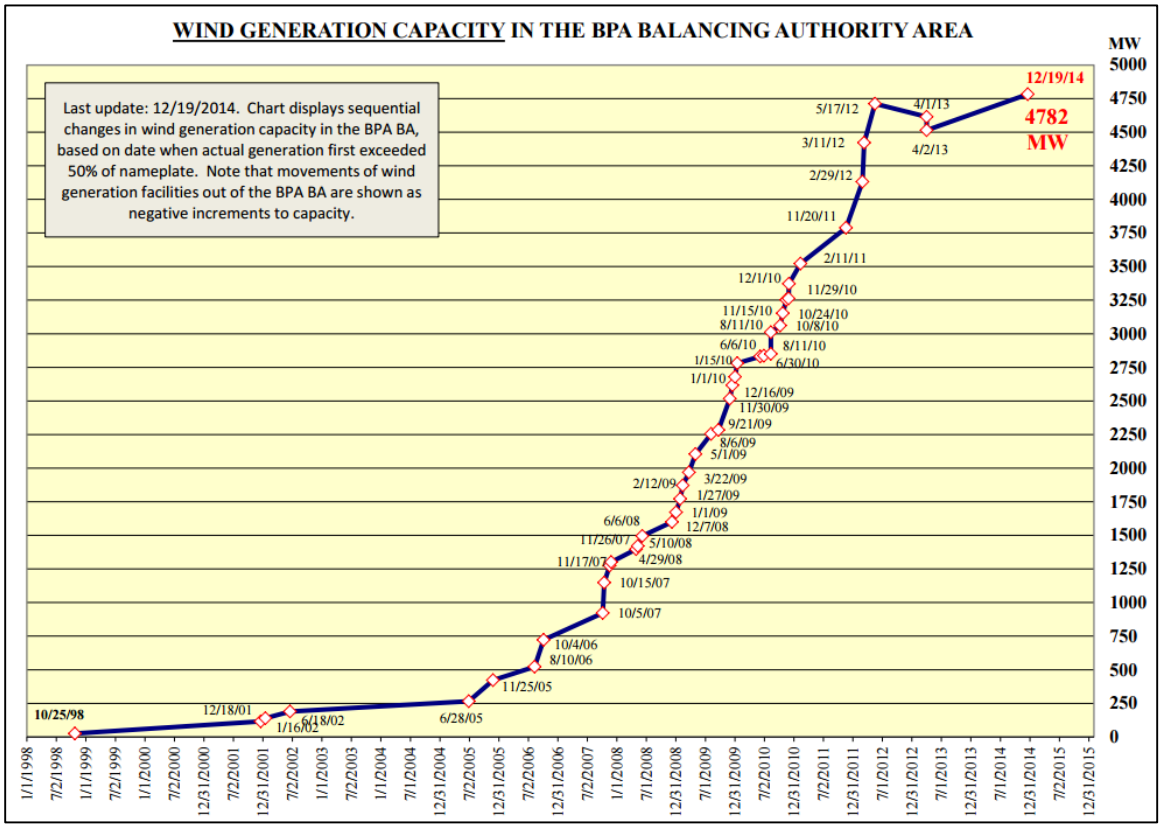

Figure 1.3: Wind growth in the BPA balancing authority area [9]. The flexibility of regional hydropower has been an important enabler of wind by providing responsive and relatively low cost reserve.

The importance of flexibility in the overall Northwest regional electric power system cannot be overstated. Not only is hydropower an important source of baseload energy, it is also commonly dispatched for load following and plays a vital role in stabilizing the system

through primary frequency response and regulation. This will be described in more detail in Chapter 2. Unfortunately though, hydropower in the Pacific Northwest and across the country is becoming increasingly less flexible, less utilized, and less available [1]. This will be demonstrated from several perspectives and serves to motivate the value of exploring adjustable speed operation to restore flexibility and better utilize emerging development opportunities.

1.1 Drivers for Change

1.1.1 Emerging Applications and Federal Initiatives to Increase Hydroelectric Power Production

The U.S. Department of Energy has set a goal of significantly increasing hydroelectric generation through the coming decade [10]. To support this goal, a large portion of the requested budget for this effort is being directed towards new development projects, particularly in the areas of existing non-powered dams, unregulated conduits, and new stream reach development projects. At the same time, new funding has been available for developers and regulatory "off-ramps" have been established by Federal Energy Regulatory Commission (FERC) for some low impact, small scale hydropower [11]. Although wind and solar have significantly outpaced hydropower in capacity additions over the last 15 years, the hydropower industry may be primed for a development boom similar to the record setting 1980s where small and medium scale projects were developed at record volume.

The regulatory and supportive policy impacting the potential development of adjustable speed hydropower can be described in part as:

- **Unit additions and upgrades at existing facilities:** A categorical tightening of operational regulations in conjunction with aging equipment have led to a significant number of unit down ratings and an overall trend of decline in the availability factor of the national hydropower system [12]. This challenges operators and system planners and decreases the cost competitiveness of

hydropower in markets where it may already be an expensive resource relative to other generation modalities. As an example, there are many cases where wind power has driven the market clearing price to historic lows on the account of the federal production tax credit which can enable wind operators to profit even at a negative price. Upgrading units to enable adjustable speed operation may be an opportunity for an industry which is already investing hundreds of millions of dollars yearly on rehabilitation and remediation to reestablish a clear market value for hydropower.

- **New generation at existing non-powered dams (NPD) and conduits:** A study conducted by the Oakridge National Laboratory found that non-powered dams could offer up to 12 GW of development potential, with roughly 75% of that resource being concentrated in a relative few federally owned lock and dam systems [13]. Additionally, conduits for irrigation, effluent streams from water processes, and other unregulated flows represent a broadly distributed opportunity for small scale hydropower with minimal environmental impact. Hydroelectric projects aimed at tapping into this potential are typically required to operate within parameters which do not materially harm the original intended function of the system. This restriction can require that a system operate through a very broad range of head and flow regimes. Adjustable speed operation could increase the system efficiency and therefore the power production relative to traditional synchronous speed units.
- **Low impact new stream development (NSD):** New stream-reach development projects represent an immense but often controversial opportunity for new development. Following the 1986 Electric Consumers Protection Act, the FERC is required to give environmental effects the same consideration that electric power production is given during permitting and relicensing [14]. As a result, NSD typically operates with no impoundment and often low available head. The lack of impoundment means that seasonal changes in flow could be significant, leading to

a wide range of operating conditions which may be best captured through adjustable speed operation.

1.1.2 Changing Water Resource Paradigms

Hydropower operators have long been able to take advantage of historical data when developing an operational strategy for the expected flow regime in a given year. For a typical dam, operators will work with water resource experts, fisheries and wildlife managers, and other subject matter experts to develop a water management strategy which can be to the level of detail of the expected number of hours of electric power production per day [15]. Typically the water used for generation is just a portion of the total water passing through the system and reflects the fact that power production is prioritized below flood control, irrigation, and fisheries and wildlife management, if applicable at a given multiuse system (Figure 1.4). Other uses include spillage to release cooling waters to reduce stress on fish during hot summer days and coordinated releases to maintain balanced water levels in a system of run-of-river projects with minimal storage (Figure 1.5).

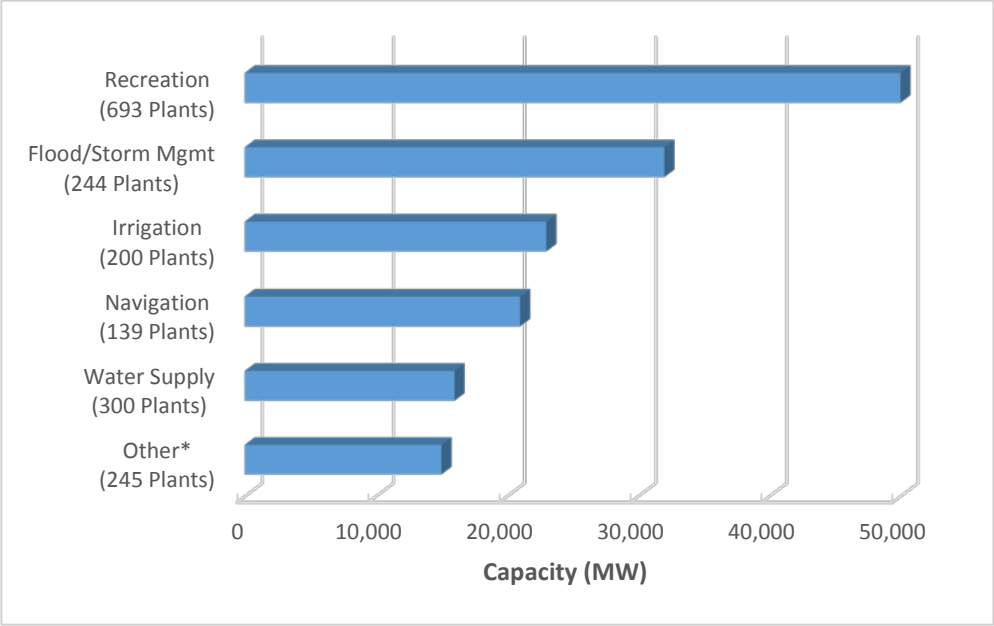

Figure 1.4: Distribution of additional functions of existing hydroelectric plants with dams [1]. The “Other” category is typically fish and wildlife pods, fire protection, or small farm ponds.

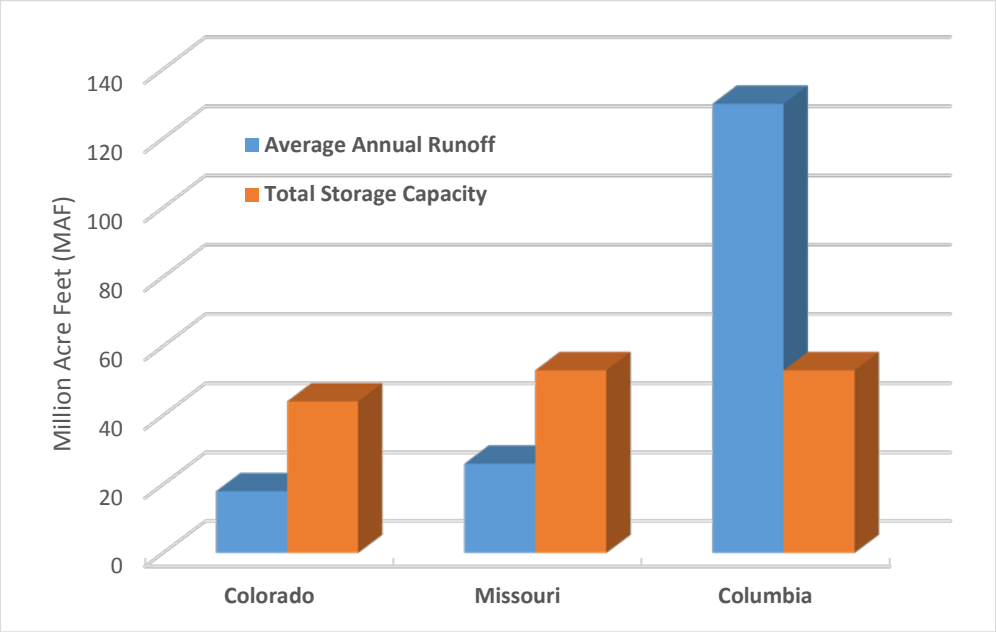

Figure 1.5: Water storage on the Columbia river system [15]. Unlike some other river systems where water storage can exceed annual runoff (*e.g.* the Colorado and Missouri rivers), the Columbia has very limited relative storage and therefore must be managed carefully to ensure sufficient water is available for all purposes at all times throughout the year.

In addition to projecting and managing expected seasonal flow regimes, operators in some regions may also need to work with flood risk managers to handle extreme weather events. The most serious risk in the Pacific Northwest comes from atmospheric rivers, commonly called a pineapple express in the region, which are capable of delivering 12 inches or more of rain per day for several days across a narrow region [16].

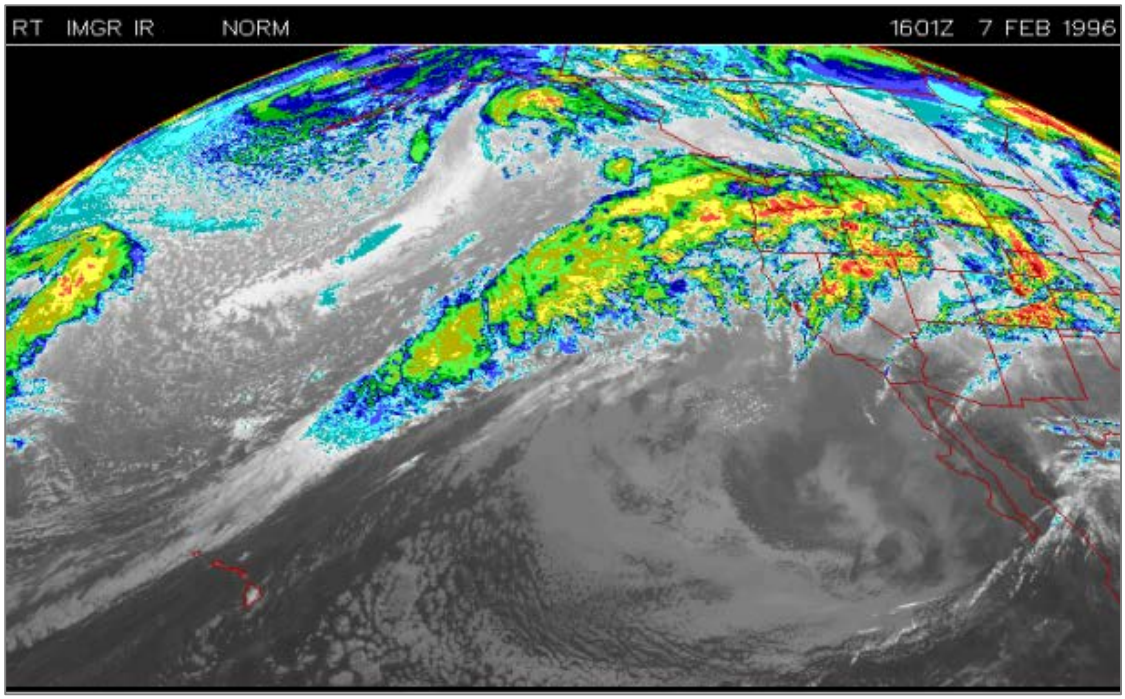

Figure 1.6: Atmospheric river making land fall over Washington State [16]. Atmospheric rivers are extreme weather events capable of delivering more than 12 inches of rain per day for several days over a very narrow region. Hydropower operators must work diligently to execute a flood risk management strategy while also respecting machine constraints.

The water flowing through a given hydropower project is often an accumulation of water draining across a broad basin. This has the effect of magnifying the impact of an atmospheric river. Regardless of the water year, atmospheric rivers have the potential to quickly overwhelm a managed system and must be aggressively mitigated regardless of the character of the given water year to minimize the risk of dam and levy overtopping. This often means passing very large volumes of water through a dam very quickly. This release must be managed such that the operating region of the unit does not include generator exclusion zones.

Taking multipurpose operation and flood risk management together, the short and long-term strategies developed and executed over the last several decades have led to very good outcomes for most stake holders in the hydropower system. Fisheries in particular have seen significant growth in returning numbers of salmon and other anadromous fish even

through drought years on the account of thoughtful water resource management (Figure 1.7).

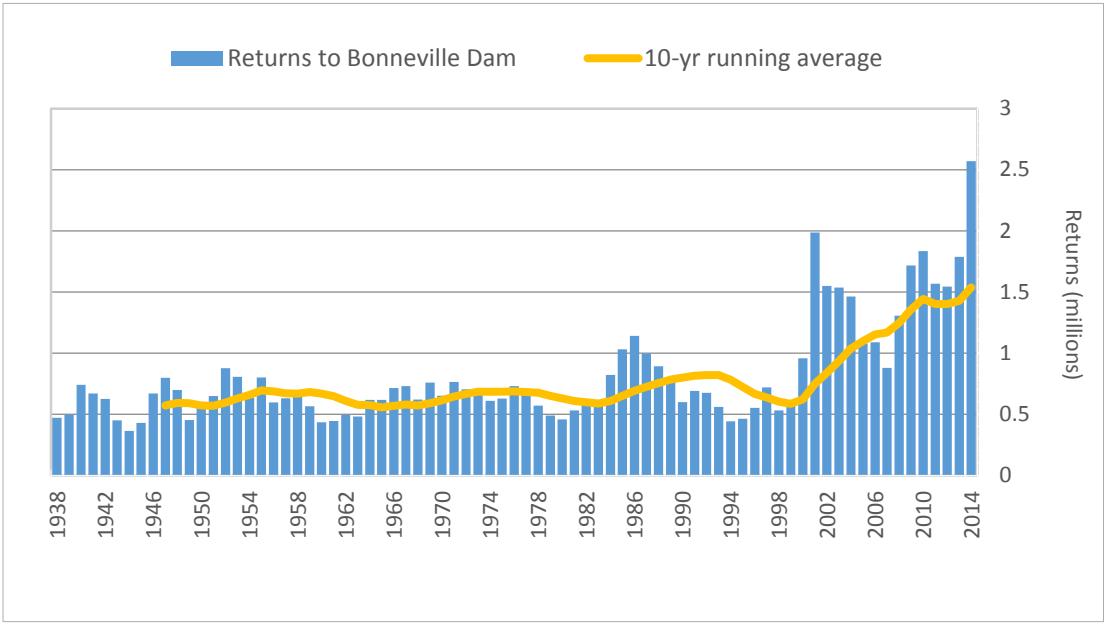

Figure 1.7: All wild and hatchery salmon and steelhead returning to the Bonneville dam in the Columbia River system [17]. Fish migration has been prioritized over electric power generation since the endangered species act of the mid 1990's and flexible hydroelectric generation can be limited during certain times of the year on that basis.

However, new information from climate experts suggests that the utility of historical models is likely to be reduced through the coming decades. Scientists researching the potential future flow regimes in the Pacific Northwest suggest that the historically defined average year is subject to change and that future flow patterns are likely to shift. Warmer temperatures are expected to result in winter rains which quickly enter the basin rather than winter snow showers which accumulate to form a snow pack which delivers, on average, 60% of the basin's water in Spring melt through May, June, and July. The impact of this change could be:

- A shift in hydroelectric power production which moves away from the typical spring peak shown in Figure 1.8 due to a lack of snow melt. The new peak would

likely align with the early spring salmon returns creating new challenges for operators who must legally prioritize fish migration over power production.

- Even greater restrictions on summer power production due to decreased water.
- August flows which are potentially below equipment rated minimums.

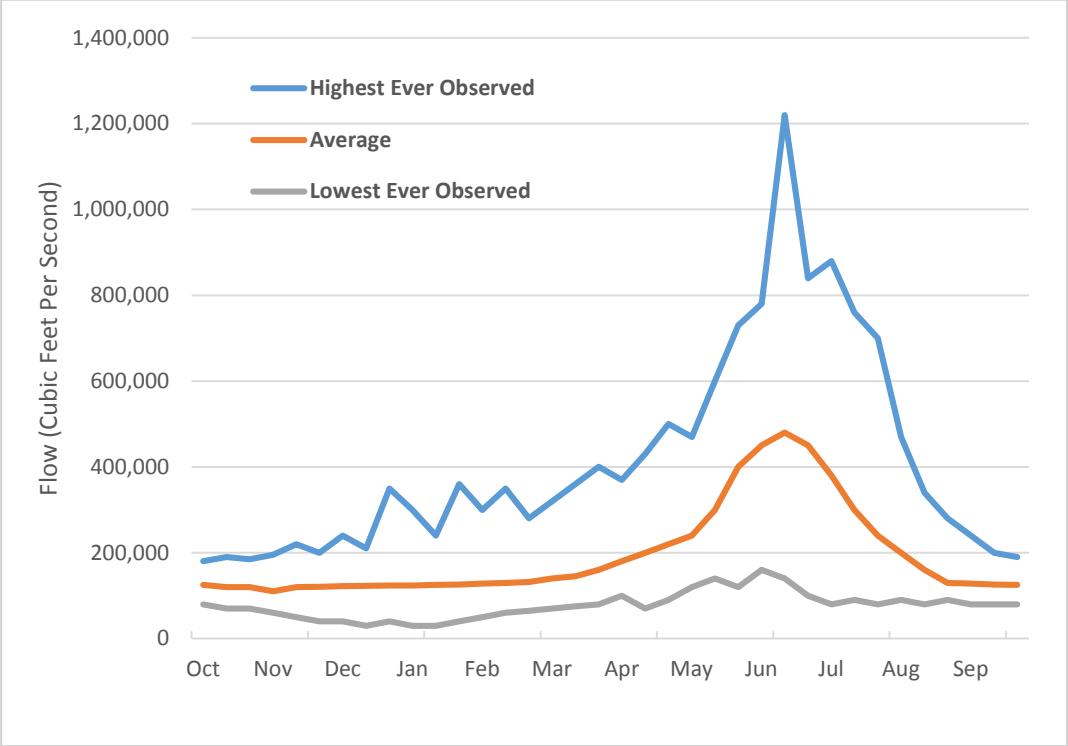

Figure 1.8: Typical river streamflows in the Columbia River as measured at The Dalles lock and dam [15]. Climate experts suggest that global warming may cause current winter snows to fall as rain in the future. This could potentially shift peak flows forward to early spring where they would then align with critical fish migration. This would be a new challenge to system operators that could limit hydroelectric flexibility.

In addition to these impacts, climate research suggest that significant droughts such as that of 2015 will become more common place. In one climate model, research suggests the drought like conditions of 2015 will become the average in the next fifty years and, even more alarming, that back-to-back major drought years may occur in the future.

Taking these important changes together, a hydropower system which can increase water use efficiency, broaden a system's operating range, and enhance grid response flexibility may be important both at small and large scale units.

1.1.3 Growth of Variable Resources and Accompanying Regional Demand and Market Changes

The generating fleet of the electric power system across the United States has undergone tremendous change over the last decade. Coal generation fell to just 38% of the national total – it had been at least 50% for decades prior to 2006 – and natural gas, wind, and utility scale solar grew significantly (Figure 1.10) [19].

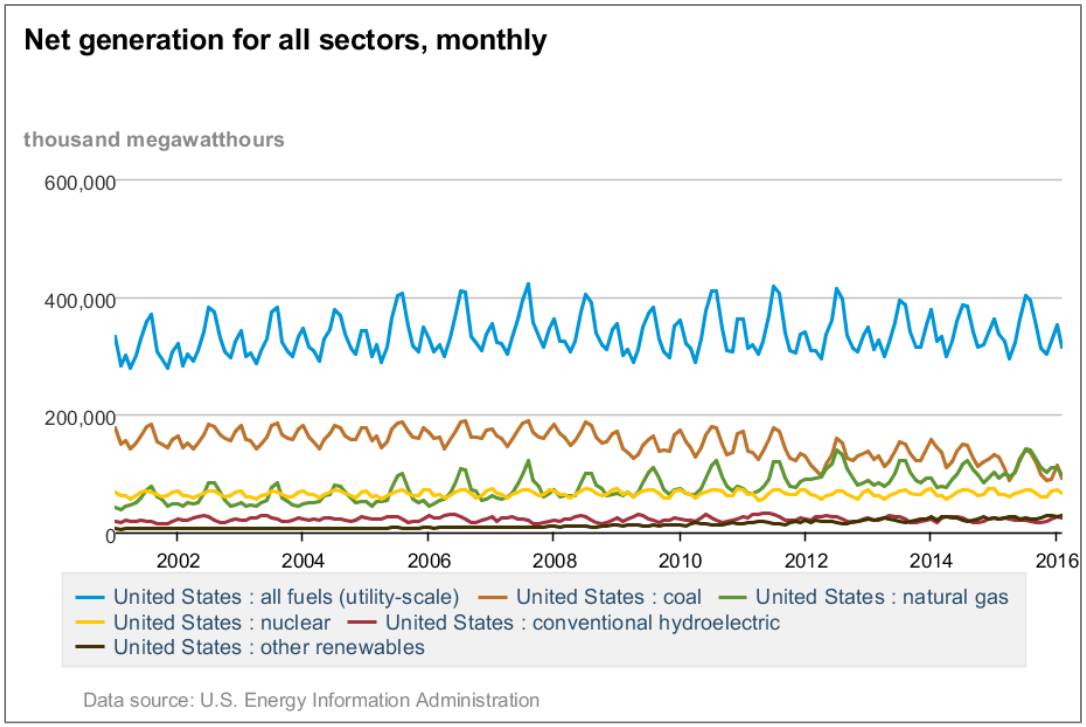

Figure 1.9: U.S. energy generation by fuel source [20]. Coal generation has followed a trend of decline which has been matched primarily by increased natural gas and non-hydroelectric renewables to result in an overall stable net total generation across.

Considering the last three years in particular, non-dispatchable variable renewable resources have combined to outpace all other sources combined in terms of new capacity

additions (Figure 1.11). The majority of these new capacity additions have been at the utility scale where the resource is bid into the electricity market, described in Chapter 2, and where reserve must also be provided by another power producer.

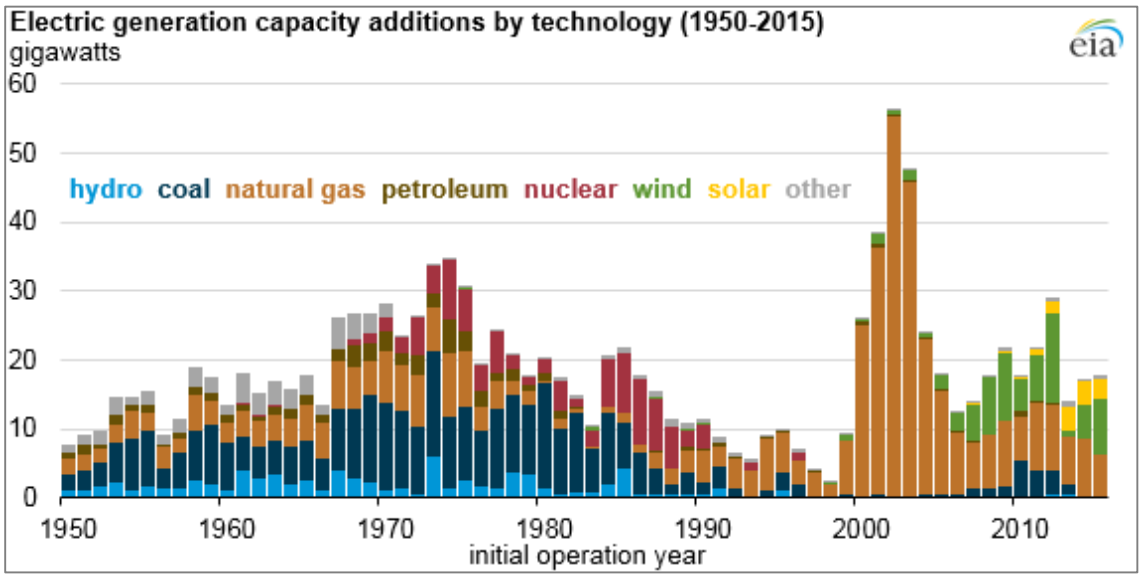

Figure 1.10: New source additions have primarily been in natural gas and non-dispatchable renewable sources over the last decade [21].

In the Pacific Northwest, hydropower has played an important role in enabling the growth of wind in particular by serving as a very flexible source of reserve which can be dispatched quickly for load following and regulation. This is especially important given that utility scale renewable energy projects are often on the order of hundreds of megawatts and can cause significant disturbances in the event of a fault or strong and unexpected period of intermittence where speed of response of stabilizing units is key.

In addition to helping to manage system disturbances, growth in western solar energy in particular has created a new paradigm, often characterized through the so called “duck curve”, where excess energy may be produced during the solar peak followed by a need for energy generation at an extraordinary ramp rate (Figure 1.12).

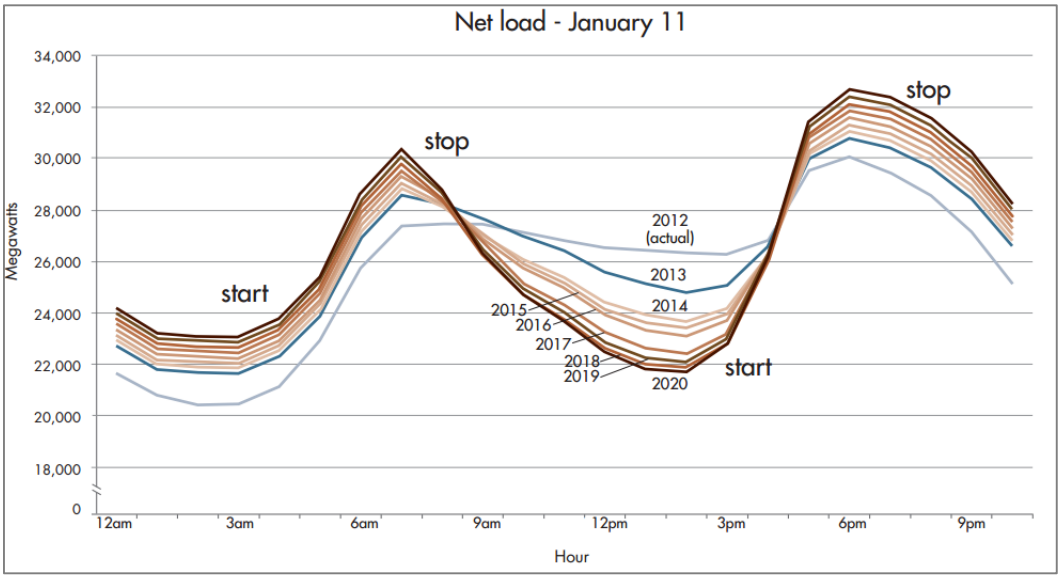

Figure 1.11: Net load curve from the California ISO [22]. Growth in non-dispatchable solar is creating a need for very flexible resources which can ramp quickly as solar generation falls before the evening demand peak.

Market tools such as the broader participation in the energy imbalance market created by CAISO may help distribute excess solar energy during peak generation. However the importance of flexible assets to manage the ramp will only increase, particularly in the southwest where utility solar growth is concentrated (Figure 1.12).

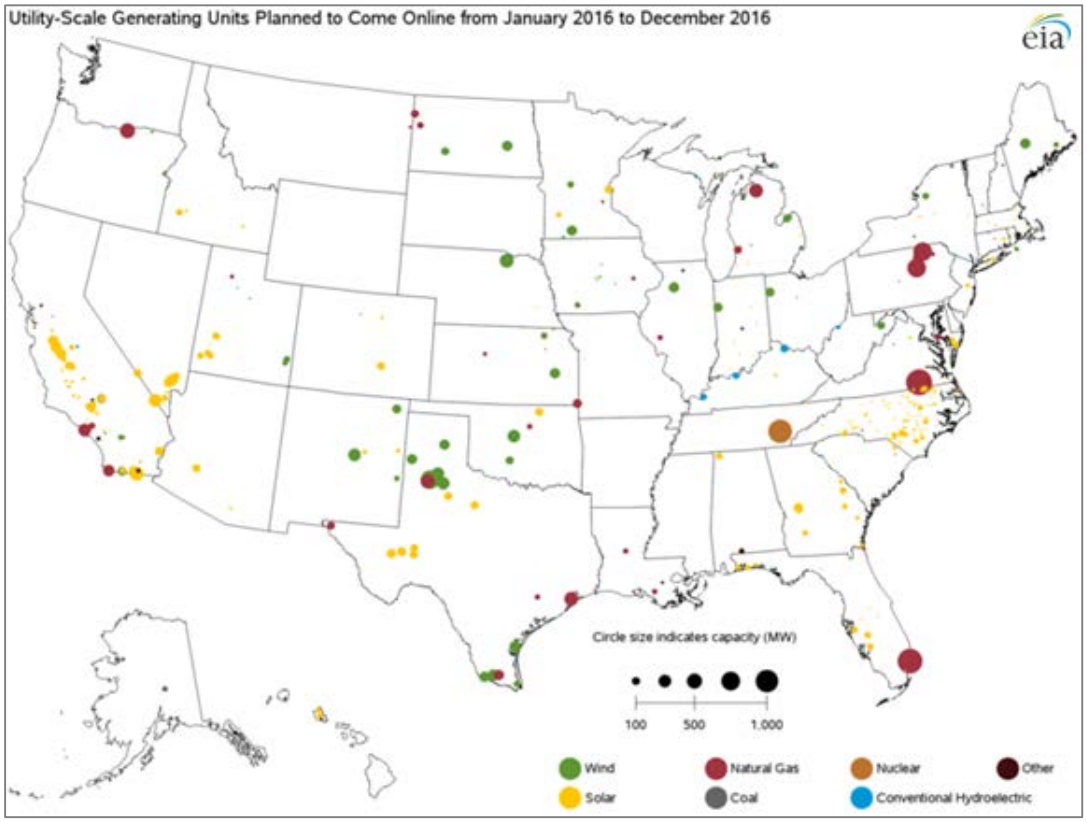

Figure 1.12: New solar growth is concentrated in the western U.S. [23]. A Northwest power system which has been built around hydroelectric power and relied on interties with California to export excess generation may face new challenges as the Western and South Western U.S. builds significant non-dispatchable solar.

Adjustable speed operation could help to ensure that a flexible hydropower resource is available to support renewable generation even in years where drought leads to challenging hydrologic operating conditions.

1.2 A Path Forward: Variable Speed Machines & Advanced Controls

Hydropower has been a reliable source of baseload and flexible power throughout the last century and has played an important role in enabling clean energy across the nation and in the west in particular. Although growth over the last decade has been minimal, the DOE hopes that financial and regulatory support will help stem this trend and potentially reinvigorate an industry which produces 5.1 jobs per MW installed. At the same time,

tightening operational regulations and emerging water resource paradigms are broadening the range of operating conditions hydropower operators may need to operate in.

Adjustable speed operation could help support new development and increase the flexibility of existing systems by broadening the range of efficient operation. Additionally, adjustable speed operation can increase the speed of response to contingencies to enable hydropower to continue to act as an important enabler of variable renewable resources. Previous work in this area has led to variable speed control systems designed to serve isolated loads through adjustable speed run of river systems [24], [25] or pumped hydropower coupled to wind generators [26]. Other studies have focused exclusively on control schemes for pumped storage in grid connected systems [27], [28]. Additionally, a significant amount of research has focused on variable speed control for axial flow systems without gates where speed is the only flow regulator [29], [30] or where gates are in place but not available for governor control [31]–[34], sometimes explicitly because of constraints on maintaining a constant forebay elevation [35]. Underlying all of this work, physical testing has shown that variable speed operation can lead to extraordinary efficiency improvements for Kaplan turbines operating below nominal head [36] and an application of variable speed systems to an effluent stream has already been proven to be successful [37].

The remainder of this document examines the market in which hydropower operates in detail before presenting the development of an adjustable speed control strategy which has been modelled in simulation and tested on hardware. The unique contribution of the control strategy developed in this work is that it is capable of improving the speed of response of a hydropower generator to help support grid stability and it can work in parallel with a traditional governor to deliver a specific set point power at the most efficient operating point. Finally, conclusions and future work will be presented and discussed.

2 Hydropower Operation and Equipment

2.1 Market for Hydroelectric Energy

The market in which hydroelectricity is sold can be a key factor in the development potential of adjustable speed hydropower. In the Pacific Northwest, the power generated from the 31 FCRPS hydroelectric dams is marketed by BPA with authority given by the Bonneville Power Act of 1937. Through this authority BPA created a 14,000 circuit-mile high voltage transmission system including the 4800 MW 500 kV AC California Oregon Intertie (COI) identified by WECC as Path 66 and an additional 3100 MW 500 kV DC link to Los Angeles identified as Path 65 [38]. The COI is composed of three total 500 kV AC lines – two built in the 1960s and the third built in the 1990s – and the HVDC line built in 1970 and upgraded throughout the following decades. BPA's current combined generation and transmission assets account for 40% of the region's total power and more than 70% of the region's high voltage lines [39].

Both the sale and transmission of energy has evolved over time as policy has driven towards an increasingly competitive market. Today, BPA acts as one of 38 balancing authorities in the Western Electricity Coordinating Council (WECC). As a balancing authority BPA is responsible for maintaining an equilibrium between load and generation in the region and can then export excess energy to other balancing authorities. Unlike many other areas which took a more aggressive approach to deregulate their markets (*i.e.* CAISO, where utilities had to sell their assets and then buy power in a true market), BPA has continued to operate a more traditional exchange using bilateral agreement for the sale of energy and transmission. In this role, utilities and high load industrial customers within the BPA balancing authority area can establish a bilateral agreement with BPA for firm power delivery.

In addition to long term contracts with BPA, regional purchasing entities as well as BPA can also purchase energy in a liquid, transparent wholesale trading hub, typically either the Mid-Columbia (mid-C) hub or the California California-Oregon Border (COB) and Nevada Oregon Border (NOB) hubs. Hydroelectricity marketed by BPA and others is a very important resource in these hubs. First, several regional utilities produce an excess of hydroelectric energy at some times through the year and are therefore supply constrained participants in the hub who need to sell their energy at any price. At the same time, growth in wind power in conjunction with support through tax incentives has enable some investor owned utilities and third party players to take advantage of low market prices for energy and provide firming through hydropower at the hub trading price.

The actual composition of the energy portfolio for regional utilities who may be participating in the hub is subject to a number of conditions including real time and future market prices, utility owned assets, risk tolerance, and more. Most utilities choose to purchase a significant portion of their energy through long term contracts and forward market agreements and operate on a day ahead market for final load shaping based on models. An example portfolio for the Eugene Water and Electric Board (EWEB) can be broadly described as a having two thirds of their supply through a power sale contract (PSC) for Tier 1 energy from BPA [40]–[44]. Half of this energy is provided as a firm block which is shaped based on historical data from a reference load year and has no additional shaping ability. The other half is provided as a slice which follows the current generation from BPA and has some ability to be shaped. The remaining one third of energy is accommodated through utility owned or long-term contracted hydropower. The majority of this resource is inflexible run-of-river generation however EWEB also owns a 114 MW with storage sufficient for 24 hours of load shaping. Like many aging hydropower assets, though, the flexibility of this resource has become increasingly limited.

Like several other mid to large size regional utilities, EWEB often has excess generation. This is processed through a real time desk which compares their scheduled generation to their actual load to generate an area control error (ACE) signal which indicates the amount of energy which can be sold on the mid-C market. Otherwise, if EWEB has a generation shortage they can passively rely on BPA to provide it at a charge with incremental cost bands based on the magnitude of power needed. Shortages less than a certain MW will be charged at the index (real time hub) price. Shortages in a band above that are charged at an index plus a percentage multiplier, and so on. This motivates utilities to accurately project their load and procure generation in advance and simplifies coordination of generating reserve.

Utilities which are smaller than EWEB often do not have a real time desk or generating assets and instead rely on a contract with BPA to manage all aspects of their supply. On the other hand, some larger utilities have developed integrated resource plans which are very unbalanced in terms of expected load *vs.* procured generation [45]. These utilities have recognized that wind and other factors have resulted in a mid-C market price which is often less than the rate for Tier 1 energy from BPA and their traders actively use the market instead of establishing long term firm contracts. Negative rates have become increasingly common on the market and reflect the inflexibility of generation assets as well as a partial consequence of strong wind growth spurred by the production tax credit which can enable wind operators to make money at a negative price [46]. This is a benefit to the purchasers at the cost of the increasingly less economic hydropower generating fleet.

2.2 Market for Ancillary Services from Flexible Resources

Flexible generators play an important role in managing energy in real time and can help owners save costs while also improving the quality of the power system. Holding capacity to respond to normal fluctuations in demand, variability in non-dispatchable resources, *etc.* is a type of ancillary service and is critical to system reliability. As shown in Figure 2.1,

this capacity is dispatched at several time scales to maintain load and generation balance under normal operation and can be delineated generally as:

- Primary Frequency Response (PFR): Automatic and autonomous response taken by the governor of an individual power plant on the order of seconds in response to sensed frequency excursions. PFR is often referred to as primary or droop control and has a goal of stabilizing the system (*i.e.* returning $\frac{df}{dt} = 0$) but will not restore grid frequency to nominal (Figure 2.2).
- Regulation: Coordinated deployment of spinning reserves held by generators under Automatic Generator Control. Initial deployment can occur within 4 seconds to eliminate the ACE and restore grid frequency to nominal on a minute-to-minute timescale [47]. Regulation through AGC is very expensive.
- Load Following: Manual dispatch of additional spinning and non-spinning (*i.e.* operational or supplemental reserve) balancing reserves on the order of minutes to economically manage intra-hour fluctuations and unload secondary reserves for subsequent re-deployment [48]. Load following is less expensive than regulation [49].

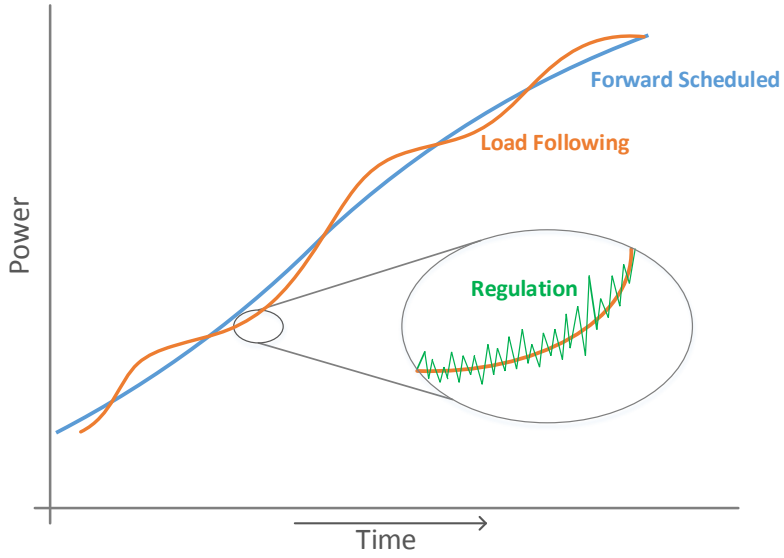

Figure 2.1: Example dispatch demonstrating that scheduled generation is supported by very responsive regulation and load following reserve to balance demand with supply on a minute-to-minute basis.

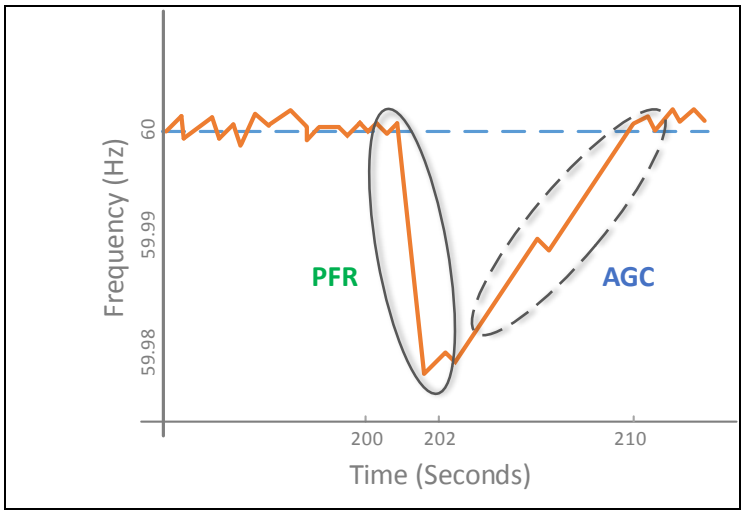

Figure 2.2: Primary frequency response (PFR) acts to stabilize the system and is followed by regulation dispatched through Automatic Generator Control to restore the grid to nominal frequency [50].

The amount of spinning and non-spinning reserve which must be held by balancing authorities in the WECC is regulated as 7% of the total load served by thermal sources plus 5% of the total load served by non-spinning sources [51]. At least half of this must be held as spinning reserve capable of loading within 10 minutes. Simply holding this reserve is an ancillary service paid by the market or the balancing authority; the energy delivered by dispatched reserves is also paid at the market rate (Figure 2.3).

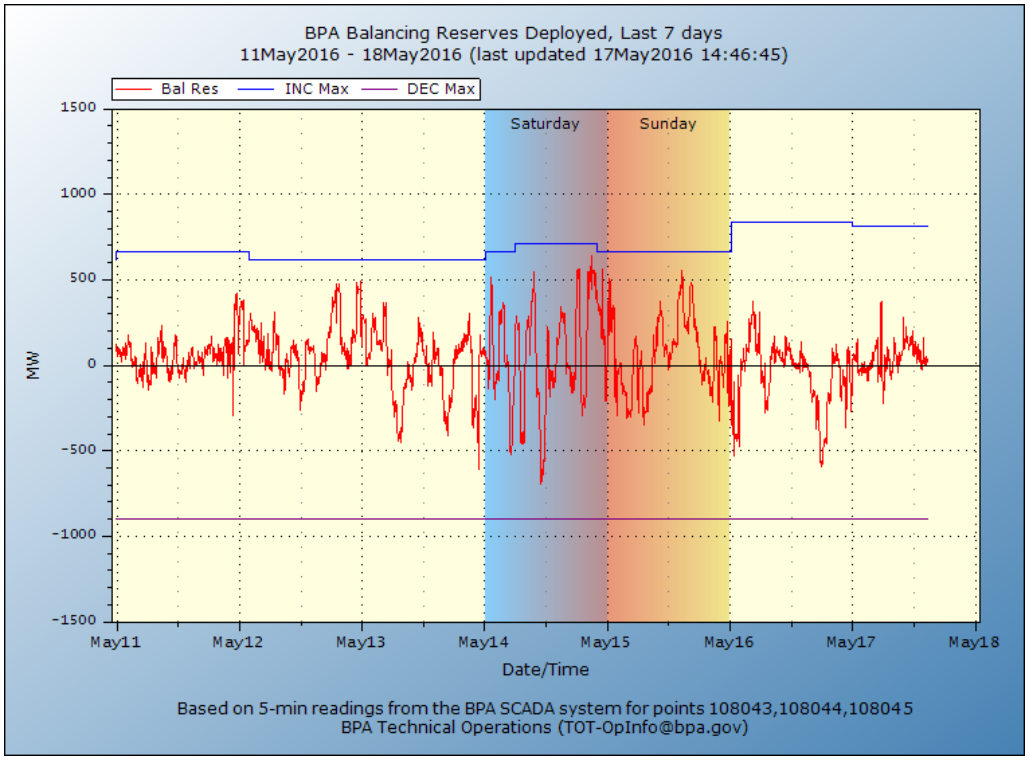

Figure 2.3: Balancing reserves held *vs.* deployed in the BPA balancing authority area.

Importantly, the speed of response of a generator providing reserve is not currently a monetized factor. For example, a coal power plant may contract or bid to provide reserve without actually being able to precisely follow the AGC signal (Figure 2.3). For this reason, more flexible resources certainly help improve system stability through improved speed of response.

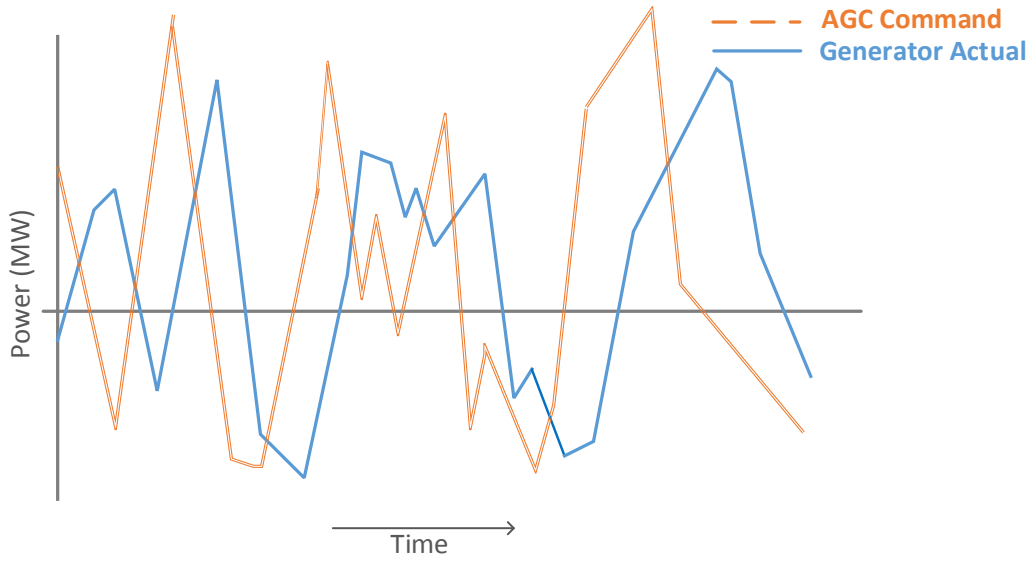

Figure 2.4: Example where a representative coal plant is not able to preciously follow the AGC command [49]. Generating units providing regulating reserve are compensated both for holding the capacity and for any actual dispatch. However, units with a slow speed of response may not be capable of ramping quickly enough to deliver the commanded dispatch.

Additionally, reserve provided by a hydropower system has the important implication of being tied to water which is often also used for many other purposes as previously described. In the highly interconnected FCRPS where operations are driven primarily by flood control and the endangered species act, providing incremental reserve draws on project storage and increases flows while decremental reserve adds storage and decreases flows [52]. This can be especially important given that court ordered specified amounts of spill during critical fish migration times can, in some years, lead BPA to disconnect some of the dams from the AGC system to avoid violating the order [53]. This can create risk in power system stability and emphasizes the importance of flexibility in the remaining units.

2.3 Typical Equipment

The control scheme developed in this work includes a model for each component in a hydropower system for simulation and hardware testing. A typical hydroelectric power

station and generating unit is shown in Figure 2.4 and Figure 2.5 and described in detail in the following subsections.

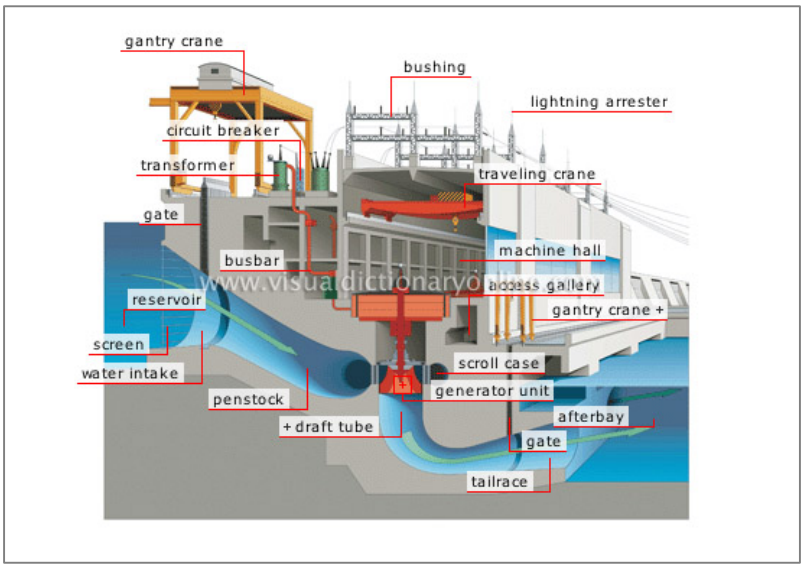

Figure 2.5: Cross-section of a hydroelectric power plant with impoundment [54]. Water flows from the reservoir, through the penstock and around the scroll case before exerting a force on the generator in a path towards the draft tube and tailrace.

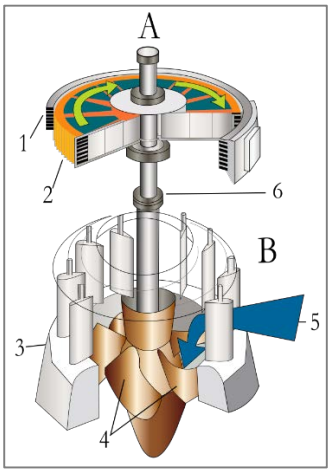

Figure 2.6: Generating unit in a hydroelectric power house [55]. Water flowing through the penstock passes through the ticket gates (3) to act on the turbine runner blade (5), turning the generator shaft (6) which spins the rotor (2) to produce electric power through the grid connected stator (1).

2.3.1 Turbine Runner

The runner of the hydropower system is the key component in converting the mechanical energy of flowing water into electrical energy to be distributed within the bulk electric power system. In large scale hydropower systems, water flowing down the penstock passes through the guide vanes - the adjustable portion of the overall flow controlling wicket gates - where it then exerts a force on the turbine runner. The turbine runner is directly connected to the electrical generator of the hydropower system. The guide vanes act as a flow control valve which can be opened or closed to create more or less mechanical power, respectively. Control of the guide vane angle is managed through the governor which is provided an external signal dictating the power to be produced.

The design of the turbine runner for large scale units is most commonly either a Francis (high head) or Kaplan (medium to low head) reaction style turbine (Figure 2.7). In very low head microhydro systems a centrifugal pump run in reverse may be used as a cost effective but relatively inefficient prime mover.

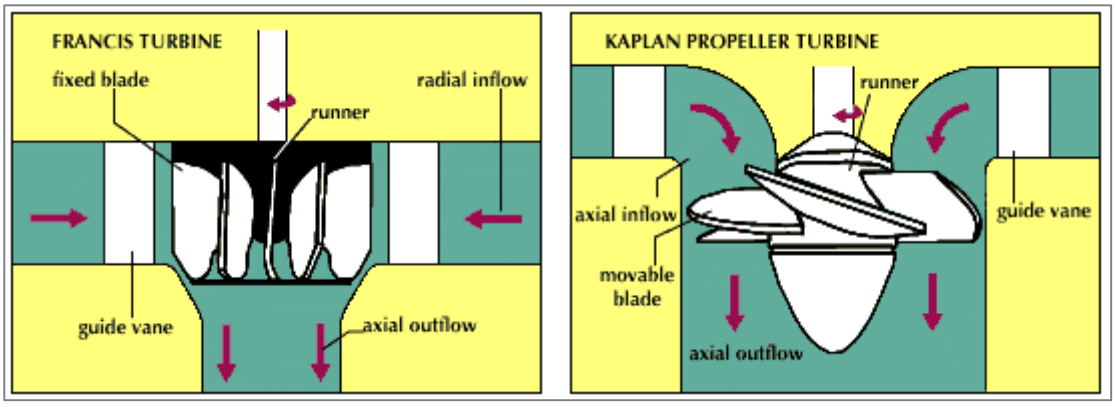

Figure 2.7: Francis *vs.* Kaplan turbine [56]. Kaplan turbines can be equipped with adjustable blades to optimize efficiency across a range of operating conditions.

Kaplans are propeller-type turbines which can be made with adjustable pitch blades to further increase efficiency under differing operating conditions. For example, each of the

22 total 23.3 foot Kaplan turbines at The Dalles dam are tuned to operate through a 30 ft. minimum *vs.* maximum head range. Typically the blade pitch controller is tuned through a procedure where the governor slowly adjusts the blade pitch throughout an entire water year under different operating conditions to determine a profile of maximum power for a given operating point.

A model of a turbine runner in a traditional system will often take gate position as an input and present the mechanical power of the turbine runner as the output. In light of improved computing power it has become common to use a non-linear approach which can account for the effects of varying flow due to gate position on effective water starting time in addition to off-nominal head. This model is often incorporated into a combined turbine, gate, and governor model for use in power system modeling tools such as PowerWorld and PSS/E. A common combined model utilized in the Pacific Northwest is referred to as HYG3 where the water column and runner are modeled as shown in Figure 2.8.

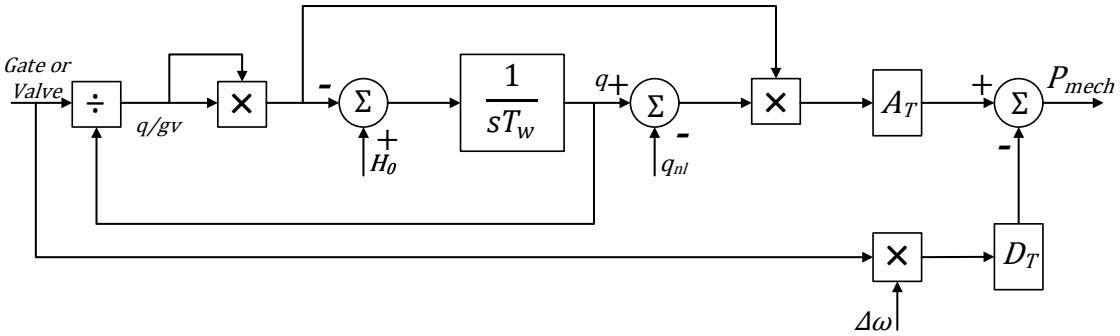

Figure 2.8: Model of the water column and turbine of a hydroelectric system. In this diagram, q is flow, gv is the gate valve position, H_0 is the nominal head, Tw is the water starting constant, q_{nl} is the no-load flow, A_t is the turbine gain, D_t is the turbine damping factor, and P_{mech} is the mechanical power from the runner acting on the generator shaft. This particular representation is a part of the IEEE HYG3 turbine/governor model and is useful for analyzing power systems containing synchronous speed units [57].

2.3.2 Governor

The governor acts as the control system to manage the active power generated by the hydropower unit. A schematic diagram of a typical modern digital governor is shown in Figure 2.9. The set point power provided to the governor comes from an outer control loop and reflects the firm market commitment as well as any adjustments made through AGC. This set-point can represent power directly or it can represent the gate position. Using a PID controller with closed loop feedback, the governor adjusts the control valve which changes the wicket gate position until the desired set-point is reached (Figure 2.10). As a note, this overall topology is very similar to the governor system for fossil fuel based turbine generators.

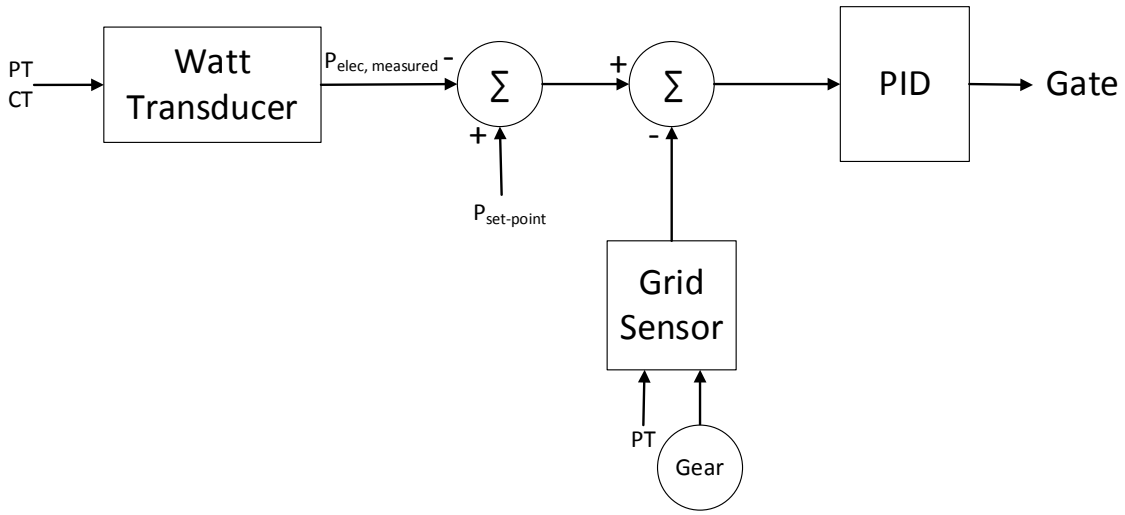

Figure 2.9: Block diagram of a typical modern digital governor for synchronous speed operation. The governor of a hydroelectric system takes a set-point gate position or power as an input and uses the gate position as the control variable to deliver the commanded value. Grid frequency excursions are measured by the governor as the generator speed of a synchronous unit and can directly change the output of the system.

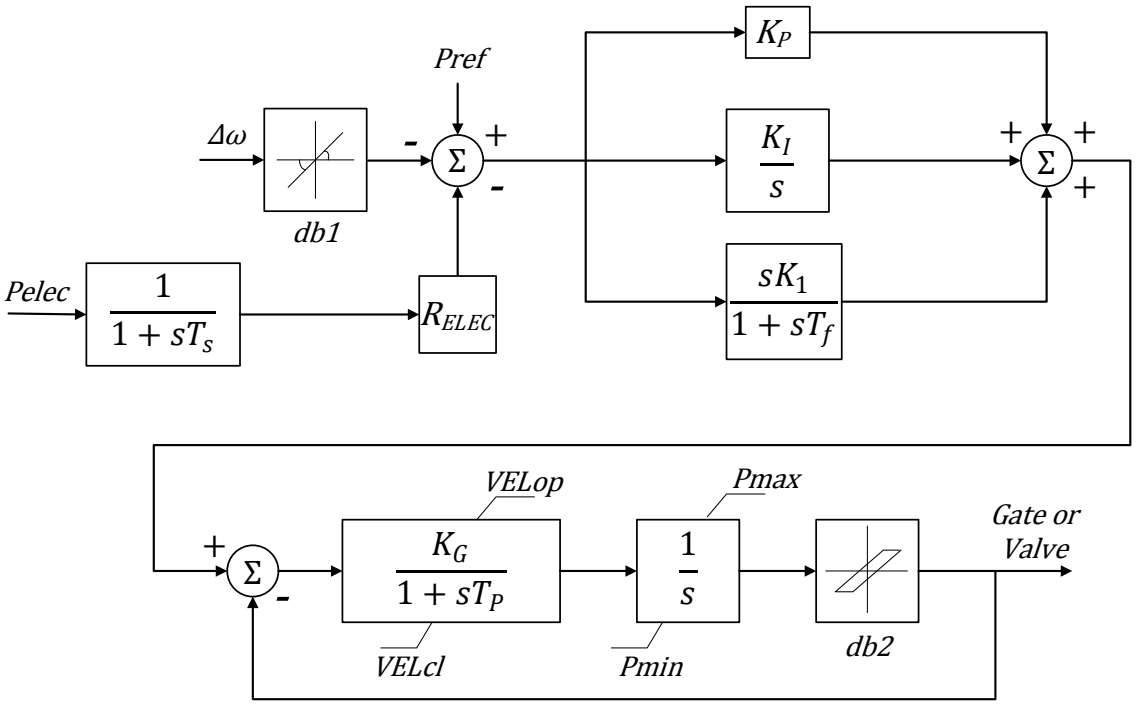

Figure 2.10: Model of governor used in HYG3 turbine governor model [57]. This is a PID system with closed loop feedback of either the gate position or measured generation at the terminal.

Using a set point value which represents gate position/unit speed is known as speed control and is common to the federally owned dams along the Columbia river due to their age. In this system, the actual gate position is fed back to the controller for closed loop feedback. Delivering a specific amount of power in MW is accomplished through a lookup table which relates gate position to power.

Using a set point value which represents power is known as load control, or also commonly speed regulation, and has become the preferred topology as it does not require a model relating gate position to power output. Instead, a watt meter at the output terminals of the electric generator is used to provide the actual power generated as closed loop feedback to the PID.

As can be seen in the previous Figure 2.10, the governor responds to changes in both the set-point value and the term $\Delta\omega$. As was described in the market section, power generating units typically provide primary frequency response, and the term $\Delta\omega$ represents the deviation from a frequency of 1.0 pu, *i.e.*

$$\Delta\omega = (speed - 1)\, pu \tag{2.1}$$

Providing frequency response through this $\Delta\omega$ term is what has been described previously as droop control and a governor is typically configured such that an excursion of $\Delta\omega = 0.05\ pu$ (*i.e.* 5%) would result in a change of 0-100% gate opening (speed control) or a 0-100% power output (load control). Typically a small deadband is used as well to limit the frequency of control action. The sum total of the set-point value and the frequency excursion term $\Delta\omega$ are processed by the PID controller to determine the gate position.

As an example, if a generating unit with 5% droop had a set point power of 0 at a given time and then sensed a frequency excursion of $\Delta\omega = 0.02\ pu$ (*i.e.* 2%) then the gate would open to 40%. Similarly, if a 100 MW unit had a firm commitment to deliver 50 MW at a given time then the P_{ref} would be set to 0.025. If a deviation of of $\Delta\omega = 0.01\, pu$ was sensed, the sum total to the reference would be 0.035 and the unit would operate at 70% of its maximum ability since 0.035 is 70% of the 0.05 droop needed to swing the output from 0 to 100%.

2.3.3 Exciter

The exciter is distinct from the governor and is used to maintain terminal voltage and power factor by providing commutated excitation to the electric generator field winding. As the machine is loaded and unloaded, the speed of a traditional unit remains constant but the current through the stator windings changes. This affects the net rotor magnetic field. The exciter is used to maintain a constant rotor field over time.

2.3.4 Electric Generator

The electric generator of a typical hydropower unit is a synchronous machine where the grid connected stator is composed of a three phase winding separated 120 electrical degrees in space in a slotted iron core made from laminations (Figure 2.11). An electrical degrees is:

$$electrical\ degrees = \frac{p}{2} * mechanical\ degrees \tag{2.2}$$

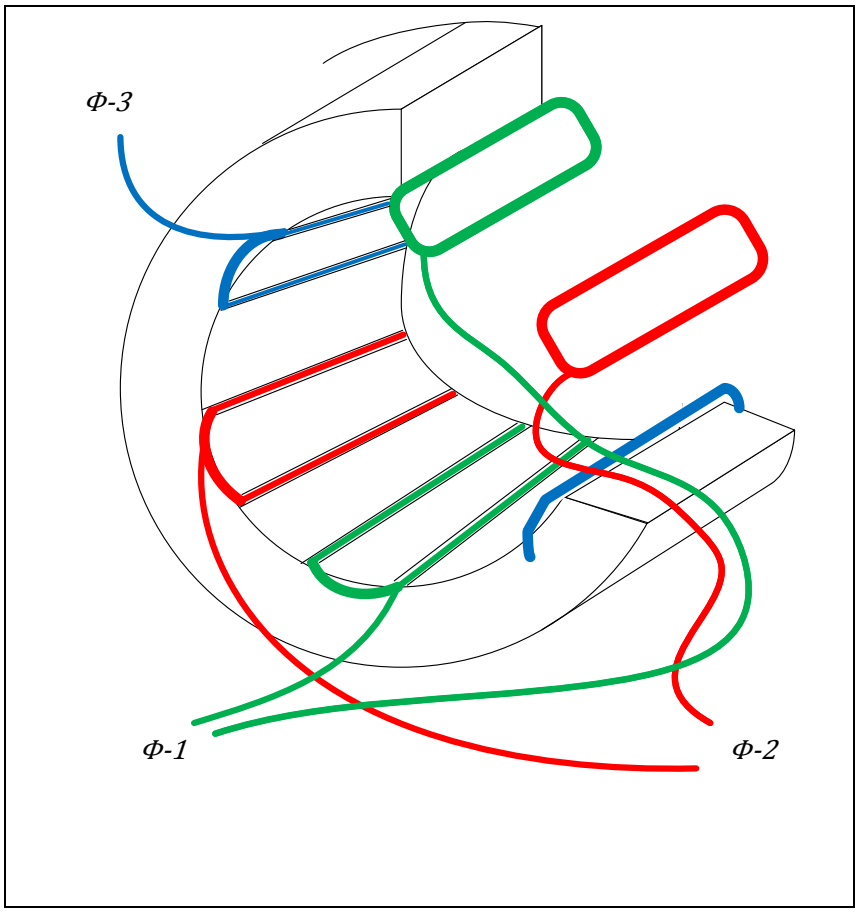

Figure 2.11: Three phase stator windings. The current carrying wires are wound into slots of the stator core.

Because of the power levels in many hydropower units, the windings are actually made of copper bars as shown in Figure 2.12 [58].

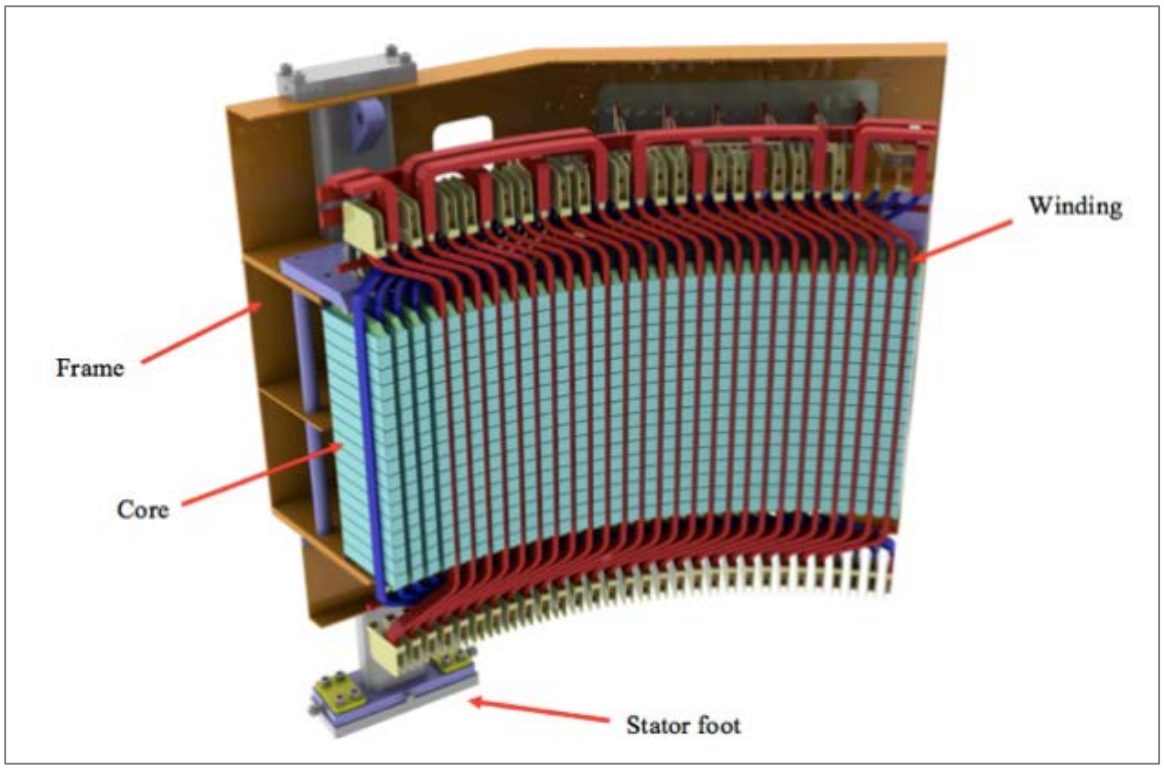

Figure 2.12: A typical hydropower stator is constructed as a core of stacked laminations with slots for solid copper bars which act as the windings [59].

Synchronous generators are characterized as being fixed speed with zero slip. A salient pole rotor as shown in Figure 2.13 is provided DC excitation through a commutator to set up a constant electromagnetic field orthogonal to the windings which spins only as the rotor itself moves. Each capped pole shown in the figure represents a pole pair of the system. This allows the hydropower unit to spin at a fixed speed per

$$RPM = \frac{2}{poles} * f * 60 \tag{2.3}$$

Figure 2.13: A salient pole rotor which would be connected to the runner shaft of the hydropower unit. Picture courtesy of Sean Brosig.

The magnitude of the field is proportional to the field current (*i.e.* rotor excitation) and is managed by the exciter as previously described such that an increased field voltage increases the field current which increases the terminal voltage at the stator. Working as a generator, torque is applied to the rotor through the runner (*i.e.* prime mover) which advances the magnetic pole of the rotor ahead relative to the axis of the stator pole (Figure 2.14). The relative angle between the rotor and stator poles is referred to as the torque or load angle such that a larger angle produces more torque. Importantly, the torque on the prime mover must not be so large that the angle opens completely and the pole pairs become unlinked. This would be referred to as slipping a pole and would likely damage a machine carrying a high load.

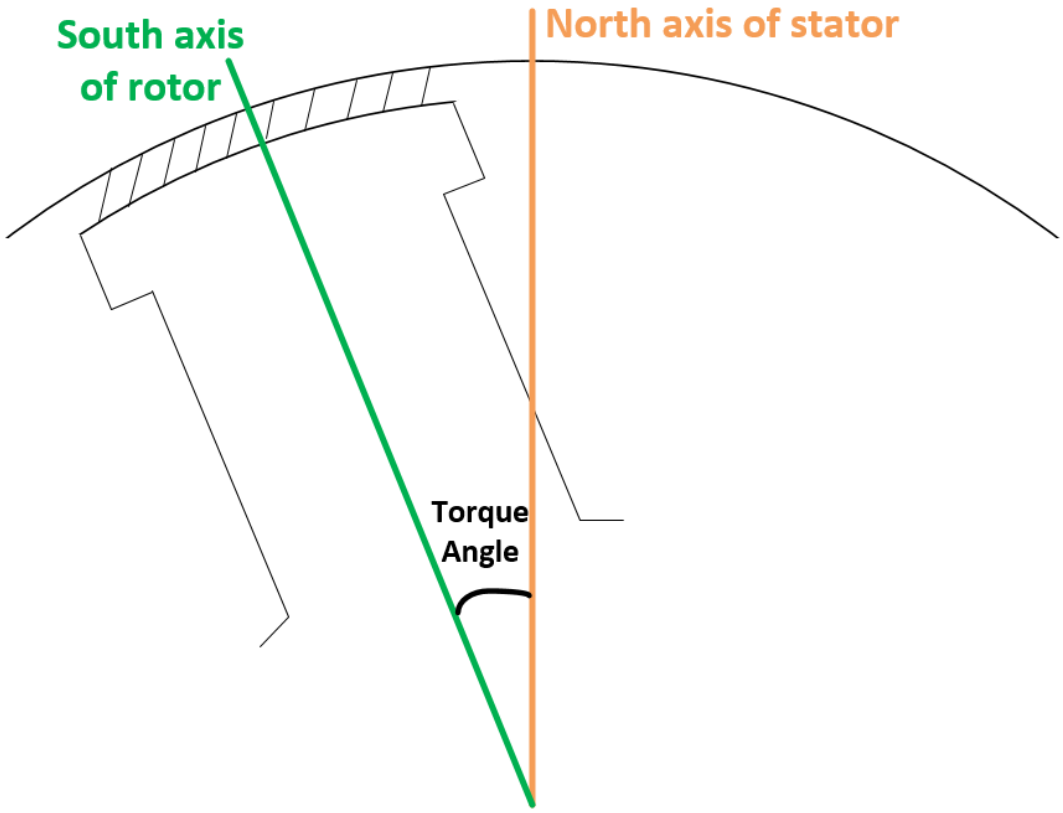

Figure 2.14: Synchronous generator operation. The rotor advanced past the axis of the stator field while still spinning at constant speed.

The outcome of being limited to a single synchronous speed is that the operating range and prime mover energy conversion efficiency is limited by the available water resource. Efficiency of a fixed speed unit is a product of head and flow alone because speed is fixed and the minimum power required to smoothly operate the unit cannot be adjusted. The latter consideration is especially important for large scale units where operating exclusion zones must be established to avoid damaging vibration and other effects (Figure 2.15). As will be discussed in a subsequent section, augmenting the rotor to enable variable speed operation can enable more efficient operation and increased speed of response.

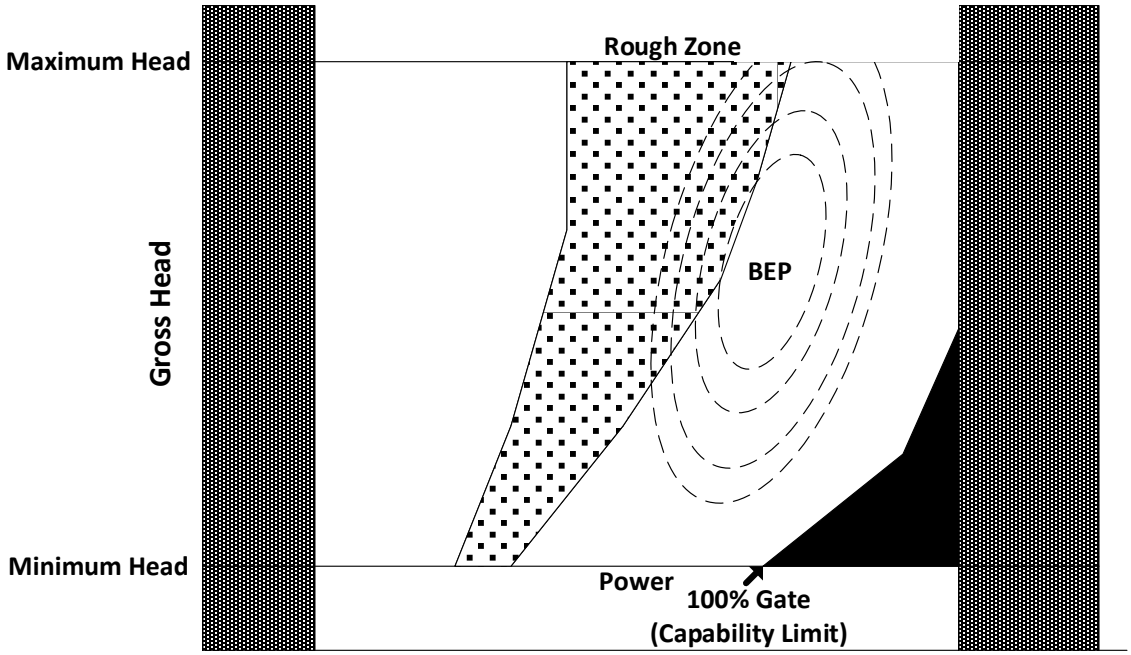

Figure 2.15: Operating zones of an example hydropower system [60]. Harmonics and hydraulic effects create rough zones which a governor must avoid or pass through quickly.

3 Variable Speed Control

The control scheme developed in this work and described in the forthcoming manuscript is broadly applicable to any machine topology where variable speed operation can be introduced. This can include an induction or synchronous machine with a variable frequency drive connected at the stator (Figure 3.1) or doubly-fed wound rotor induction generator (DFIG) with a grid connected stator and a power converter connected rotor (Figure 3.2).

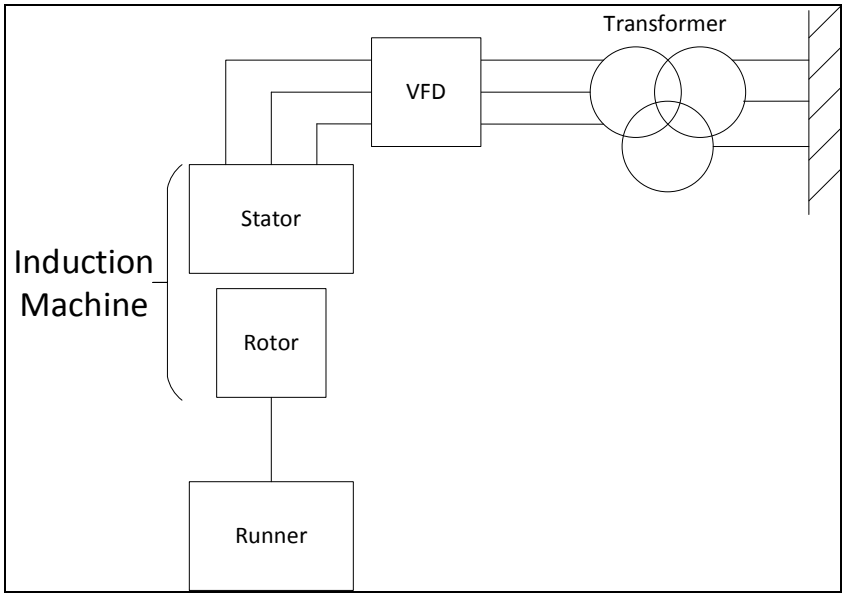

Figure 3.1: Block diagram demonstrating a variable speed system built upon a stator connected variable frequency drive.

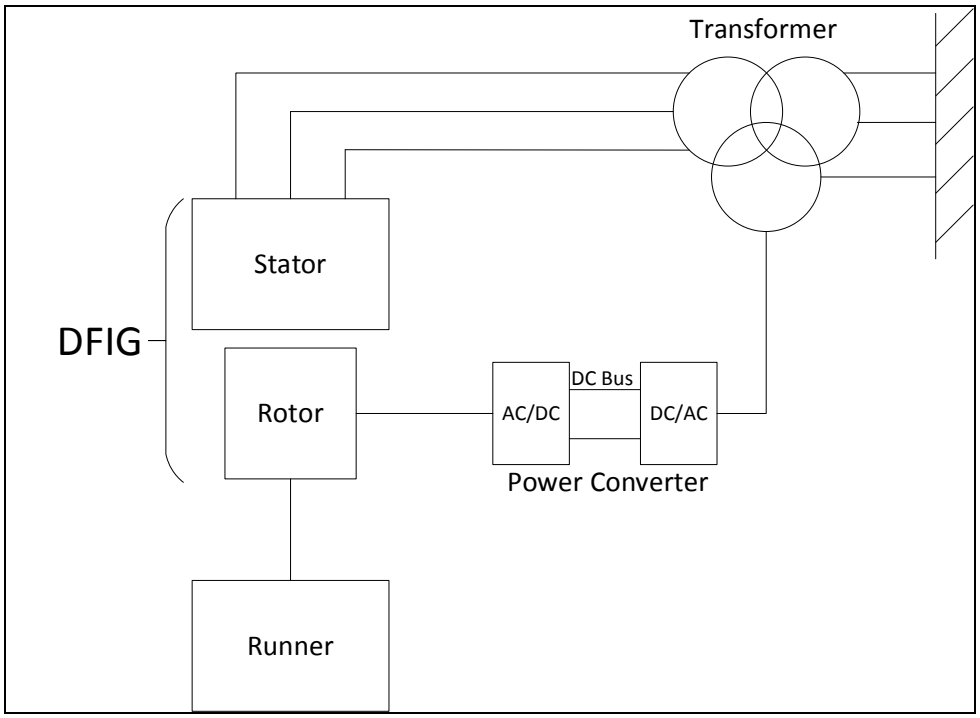

Figure 3.2: Block diagram demonstrating a variable speed system built upon doubly fed wound rotor induction generator (DFIG).

A stator connected variable frequency drive (VFD) is the simplest topology and would be appropriate for small scale hydropower projects which can use commercially available VFDs capable of handling the full rated power of the generating system. Hydroelectric projects at medium and large scale can be on the order of MWs to hundreds of MWs are therefore not good candidates for VFD connection given the need for the stator connected drive to handle the entire rated power of the system. Instead, DFIG generators common to the wind industry are more suitable because they utilize a rotor connected power converter, commonly through a back-to-back AC/DC converter, which is only required to handle the slip power of the machine. Depending on the application, this could be between 5-20%.

As will be shown in Chapter 4, the adjustable speed control scheme developed in this work was tested in simulation using a DFIG topology with rotor speed control and was evaluated

on hardware using a stator connected VFD. In this way, the simulation results represent a potential large scale application and the hardware results are representative of a potential small scale hydroelectric system.

3.1 Doubly Fed Induction Generator (DFIG) - Machine and Control

A block diagram of the overall model for simulation and control is shown in Figure 3.3 and serves to illuminate in advance the role of each of the forthcoming derivations.

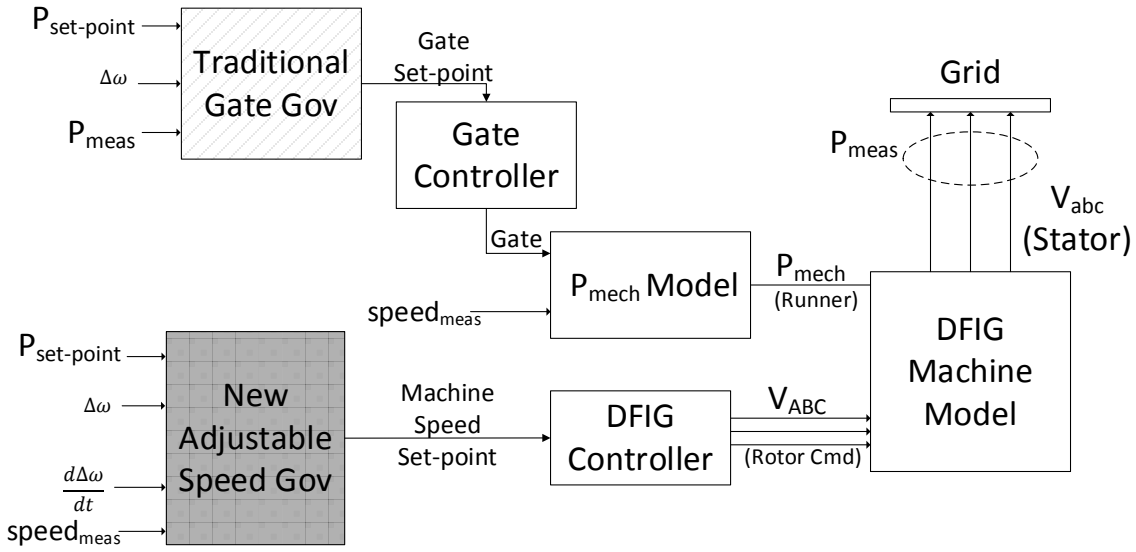

Figure 3.3: Block diagram of overall model for simulation and control using a DFIG.

3.1.1 Machine Model

The DFIG model utilized in this work was developed according to [61] and is described with the fundamental equations,

Stator:

$$v_{as} = r_{as} i_{as} + \frac{d\lambda_{as}}{dt} \tag{3.1}$$

$$v_{bs} = r_{bs} i_{bs} + \frac{d\lambda_{bs}}{dt} \tag{3.2}$$

$$v_{cs} = r_{cs} i_{cs} + \frac{d\lambda_{cs}}{dt} \tag{3.3}$$

Rotor:

$$v_{AR} = r_{AR} i_{AR} + \frac{d\lambda_{AR}}{dt} \tag{3.4}$$

$$v_{BR} = r_{BR} i_{BR} + \frac{d\lambda_{BR}}{dt} \tag{3.5}$$

$$v_{CR} = r_{CR} i_{CR} + \frac{d\lambda_{CR}}{dt} \tag{3.6}$$

where each term r represents the winding resistance for the respective phase and each term $\frac{d\lambda}{dt}$ represents the time rate of change in flux linkage.

Tracking the term $\frac{d\lambda}{dt}$ is very complex because the flux linking each phase is a function of mutual inductance between the stator and rotor, cross-cutting from multiple phase currents at the same time, and a position (θ) dependent inductance, *i.e.*

$$\frac{d\lambda}{dt} = f(i_{as}, i_{bs}, i_{cs}, i_{AR}, i_{BR}, i_{CR}, \theta) \tag{3.7}$$

This can be written explicitly for the stator as

$$\begin{bmatrix} \lambda_{as} \\ \lambda_{bs} \\ \lambda_{cs} \end{bmatrix} = \begin{bmatrix} \lambda_{as(s)} \\ \lambda_{bs(s)} \\ \lambda_{cs(s)} \end{bmatrix} + \begin{bmatrix} \lambda_{as(r)} \\ \lambda_{bs(r)} \\ \lambda_{cs(r)} \end{bmatrix} \tag{3.8}$$

where the subscripts of (s) and (r) indicate the contribution from the stator and the rotor respectively,

$$\begin{bmatrix} \lambda_{as(s)} \\ \lambda_{bs(s)} \\ \lambda_{cs(s)} \end{bmatrix} = \begin{bmatrix} L_{AA} & L_{AB} & L_{AC} \\ L_{BA} & L_{BB} & L_{BC} \\ L_{CA} & L_{CB} & L_{CC} \end{bmatrix} \begin{bmatrix} i_{as} \\ i_{bs} \\ i_{cs} \end{bmatrix} \tag{3.9}$$

$$\begin{bmatrix} \lambda_{as(r)} \\ \lambda_{bs(r)} \\ \lambda_{cs(r)} \end{bmatrix} = \begin{bmatrix} M_{as.Ar} & M_{as.Br} & M_{as.Cr} \\ M_{bs.Ar} & M_{bs.Br} & M_{bs.Cr} \\ M_{cs.Ar} & M_{cs.Br} & M_{cs.Cr} \end{bmatrix} \begin{bmatrix} i_{ar} \\ i_{br} \\ i_{cr} \end{bmatrix} \tag{3.10}$$

A model could be developed to track each of these terms as state variables however it is much more straight forward to use a reference frame transformation to abstract the actual phase windings into the orthogonal dq windings (Figure 3.4).

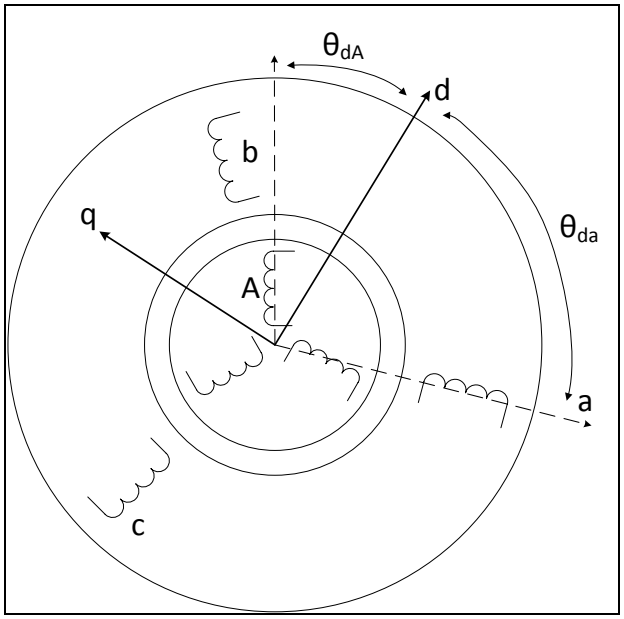

Figure 3.4: Visual representation of machine windings in the ABC and dq reference frames.

The development of the dq reference frame transformation begins by assuming three phase excitation with a 120° electrical phase shift, *i.e.*

Stator:

$$v_{as} = r_{as} i_{as} + \frac{d\lambda_{as}}{dt} * e^{j0^{\circ}} \tag{3.11}$$

$$v_{bs} = r_{bs} i_{bs} + \frac{d\lambda_{bs}}{dt} * e^{j120^{\circ}} \tag{3.12}$$

$$v_{cs} = r_{cs} i_{cs} + \frac{d\lambda_{cs}}{dt} * e^{j-120^{\circ}} \tag{3.13}$$

and likewise for the rotor.

A space vector for the stator and rotor can then be defined as

$$\overrightarrow{v_s} = r_s \overrightarrow{\imath_s} + \frac{d}{dt} \overrightarrow{\lambda_s} \tag{3.14}$$

$$\overrightarrow{v_r} = r_r \overrightarrow{\imath_r} + \frac{d}{dt} \overrightarrow{\lambda_r} \tag{3.15}$$

Using the previous Figure 3.4 we can note the relationship between the actual system and the dq reference frame can be given as

$$\overrightarrow{v_s^d} = \overrightarrow{v_s} e^{-j\theta_d} \tag{3.16}$$

where the superscript *d* represents the stator space vector with respect to the *d* axis.

Dividing both sides by $e^{-j\theta_d}$

$$\overrightarrow{v_s^d} e^{j\theta_d} = r_s \overrightarrow{\imath_s^d} e^{j\theta_d} + \frac{d}{dt} \overrightarrow{\lambda_s^d} e^{j\theta_d} \tag{3.17}$$

$$\overrightarrow{v_s^d} e^{j\theta_d} = r_s \overrightarrow{\imath_s^d} e^{j\theta_d} + e^{j\theta_d} \frac{d}{dt} \overrightarrow{\lambda_s^d} + \overrightarrow{\lambda_s^d} j\omega e^{j\theta_d} \tag{3.18}$$

$$\overrightarrow{v_s^d} = r_s \overrightarrow{\imath_s^d} + \frac{d}{dt} \overrightarrow{\lambda_s^d} + j\omega \overrightarrow{\lambda_s^d} \tag{3.19}$$

Given that the q axis is 90° ahead of d,

$$v_{sd} + jv_{sq} = r_s(i_{sd} + ji_{sq}) + \frac{d}{dt}(\lambda_{sd} + \lambda_{sq}) + (j\omega_d\lambda_{sd} - \omega_d\lambda_{sq}) \tag{3.20}$$

Finally,

$$v_{sd} = r_s i_{sd} + \frac{d}{dt}\lambda_{sd} - \omega_d\lambda_{sq} \tag{3.21}$$

$$v_{sq} = r_s i_{sq} + \frac{d}{dt}\lambda_{sq} + \omega_d\lambda_{sd} \tag{3.22}$$

$$v_{rd} = r_r i_{rd} + \frac{d}{dt}\lambda_{rd} - \omega_{dA}\lambda_{rq} \tag{3.23}$$

$$v_{rq} = r_r i_{rq} + \frac{d}{dt}\lambda_{rq} + \omega_{dA}\lambda_{rd} \tag{3.24}$$

In this expression, the flux linkage can be calculated as

$$\lambda_{sd} = (L_{ls} + L_m)i_{sd} + L_m i_{rd} \tag{3.25}$$

$$\lambda_{sq} = \underbrace{(L_{ls} + L_m)}_{L_s} i_{sq} + L_m i_{rq} \tag{3.26}$$

$$\lambda_{rd} = (L_{lr} + L_m)i_{rd} + L_m i_{sd} \tag{3.27}$$

$$\lambda_{rq} = \underbrace{(L_{lr} + L_m)}_{L_r} i_{rq} + L_m i_{sq} \tag{3.28}$$

Which can be written in matrix form as

$$\begin{bmatrix}\lambda_{sd}\\ \lambda_{sq}\\ \lambda_{rd}\\ \lambda_{rq}\end{bmatrix} = \underbrace{\begin{bmatrix}L_s & 0 & L_m & 0\\ 0 & L_s & 0 & L_m\\ L_m & 0 & L_r & 0\\ 0 & L_m & 0 & L_r\end{bmatrix}}_{M}\begin{bmatrix}i_{sd}\\ i_{sq}\\ i_{rd}\\ i_{rq}\end{bmatrix} \tag{3.29}$$

At this point it is possible to directly write the fundamental equations used in the DFIG model. First, from (3.19),

$$\begin{bmatrix} v_d \\ v_q \end{bmatrix} = \sqrt{\frac{2}{3}} \begin{bmatrix} cos(\theta_{da}) & cos(\theta_{da} - \frac{2\pi}{3}) & cos(\theta_{da} - \frac{4\pi}{3}) \\ -sin(\theta_{da}) & -sin(\theta_{da} - \frac{2\pi}{3}) & -sin(\theta_{da} - \frac{4\pi}{3}) \end{bmatrix} \begin{bmatrix} v_a(t) \\ v_b(t) \\ v_c(t) \end{bmatrix} \quad (3.30)$$

From Figure 3.4, this expression can also be used for rotor values by using θ_{dA}. This expression can also be used interchangeably with current by replacing all voltage terms with currents.

Then, using (3.21) and (3.22),

$$\frac{d}{dt}\begin{bmatrix} \lambda_{sd} \\ \lambda_{sq} \end{bmatrix} = \begin{bmatrix} v_{sd} \\ v_{sq} \end{bmatrix} - R_s \begin{bmatrix} i_{sd} \\ i_{sq} \end{bmatrix} - \omega_d \begin{bmatrix} 0 & -1 \\ 1 & 0 \end{bmatrix} \begin{bmatrix} \lambda_{sd} \\ \lambda_{sq} \end{bmatrix} \quad (3.31)$$

Considering this expression in detail and from a controls perspective, the flux linkage λ is a state variable and can be tracked directly, the voltages v are provided externally as actual phase values at known values which can be converted to dq through (3.30), and the currents i can be calculated *via* (3.30) as

$$\begin{bmatrix} i_{sd} \\ i_{sq} \\ i_{rd} \\ i_{rq} \end{bmatrix} = M^{-1} \begin{bmatrix} \lambda_{sd} \\ \lambda_{sq} \\ \lambda_{rd} \\ \lambda_{rq} \end{bmatrix} \quad (3.32)$$

At this point, all values associated with the stator can be calculated and the only unknown value for the rotor is the angle. This derivative of angle is speed, and rotor mechanical speed can be calculated through torque.

Torque on the rotor d axis is a result of q axis flux interacting with current carrying wires on the d axis.

$$T_{d,rotor} = \frac{P}{2}\left(L_m i_{sq} + L_r i_{rq}\right) i_{rd} = \frac{P}{2} \lambda_{rq} i_{rd} \quad (3.33)$$

Similarly, q axis torque is produced by d axis flux. This torque on the rotor is clockwise and, accordingly, carries a negative sign.

$$T_{q,rotor} = -\frac{P}{2}(L_m i_{sd} + L_r i_{rd}) i_{rq} = -\frac{P}{2}\lambda_{rd} i_{rq} \tag{3.34}$$

In combination,

$$T_{em} = T_{d,rotor} + T_{q,rotor} = \frac{P}{2} L_m \left(i_{sq} i_{rd} - i_{sd} i_{rq}\right) = \frac{P}{2}(\lambda_{rq} i_{rd} - \lambda_{rd} i_{rq}) \tag{3.35}$$

Then, working towards an expression for the rotor mechanical speed, w_{mech}

$$\frac{d}{dt}\omega_{mech} = \frac{T_{em} - T_L}{J_{eq}} \tag{3.36}$$

Which is related to the rotor electrical speed in rad/sec as

$$\omega_m = \frac{P}{2}\omega_{mech} \tag{3.37}$$

Through the key expressions of (3.31), (3.32), and (3.35) a model for the DFIG can be developed. For a grid connected generator, $V_{abc}/V_{s,dq}$ are grid voltages and $V_{ABC}/V_{r,dq}$ represent the control input as previously shown in Figure 3.3. The development of the controller to take a reference speed and convert it to dq voltages to be applied by the rotor converter is described in the next subsection.

3.1.2 Speed Control Loop

The control scheme developed as a part of this work calculates a reference set-point speed for a hydropower system to operate at. For a DFIG unit this corresponds to the rotor speed and it is achieved via $V_{r,dq}$ applied through the rotor connected power converter. This section develops the control strategy based on [62] to follow a reference speed.

Assuming stator voltage oriented control, $v_{rq}^*$is proportional to reactive power, Q_s^*, and is useful for power factor management. Similarly, v_{rd}^* is proportional to ω_r^* and is useful for

active power management and controlling the speed of the rotor relative to the synchronous speed, ω_{dA}.

For the purpose of speed control the expressions of the form in (3.21)(3.22) can be combined with (3.29) to be written in expanded form as

$$v_{rq} = r_r i_{rq} + \frac{d}{dt}(L_r i_{rq} + L_m i_{sq}) + \omega_{dA}(L_r i_{rd} + L_m i_{sd}) \tag{3.38}$$

Expanding (3.32) on the stator dependent terms,

$$i_{sd} = \frac{\lambda_{sd}}{L_s} - \frac{L_m}{L_s} i_{rd} \tag{3.39}$$

$$i_{sq} = \frac{\lambda_{sq}}{L_s} - \frac{L_m}{L_s} i_{rq} \tag{3.40}$$

Assuming stator flux transients are negligible,

$$\frac{d}{dt}\lambda_{sq} = \frac{d}{dt}\left(L_s i_{sq} + L_m i_{rq}\right) = 0 \tag{3.41}$$

$$\frac{d}{dt} i_{sq} = -\frac{L_m}{L_s}\frac{d}{dt} i_{rq} \tag{3.42}$$

Combining to form an expression which is only dependent on rotor current,

$$v_{rq} = r_r i_{rq} + \left[L_r + L_m\left(-\frac{L_m}{L_s}\right)\right]\frac{d}{dt} i_{rq} + \omega_{dA}\left[L_r i_{rd} + L_m(\frac{\lambda_{sd}}{L_s} - \frac{L_m}{L_s} i_{rd})\right] \tag{3.43}$$

Simplifying through factorization of the last term,

$$v_{rq} = r_r i_{rq} + \left(L_r - \frac{L_m^2}{L_s}\right)\frac{d}{dt} i_{rq} + \omega_{dA} i_{rd}\left(L_r - \frac{L_m^2}{L_s}\right) + \omega_{dA}\frac{L_m}{L_s}\lambda_{sd} \tag{3.44}$$

Defining a temporary term,

$$\sigma = 1 - \frac{L_m^2}{L_s L_r} \tag{3.45}$$

and combining (3.44) and (3.45),

$$v_{rq} = r_r i_{rq} + L_r \sigma \frac{d}{dt} i_{rq} + \omega_{dA} i_{rd} L_r \sigma + \omega_{dA} \frac{L_m}{L_s} \lambda_{sd} \tag{3.46}$$

The last term, λ_{sd}, can be assumed constant for a small signal transfer function converting q axis voltage to current. This enables it to be removed from the expression as it is not affected by changes in rotor q axis current, *i.e.*

$$v_{rq} = r_r i_{rq} + L_r \sigma \frac{d}{dt} i_{rq} + \omega_{dA} i_{rd} L_r \sigma \tag{3.47}$$

Using the similarity shown in (3.23) and (3.24),

$$v_{rd} = r_r i_{rd} + L_r \sigma \frac{d}{dt} i_{rd} - \omega_{dA} i_{rq} L_r \sigma \tag{3.48}$$

The last terms can be fed forward to develop an expression for $i_{rq}^*$from the set-point speed to leave

$$\frac{I_{rq}(s)}{V_{rq}(s)} = \frac{1}{r_r + sL_r\sigma} \tag{3.49}$$

$$\frac{I_{rd}(s)}{V_{rd}(s)} = \frac{1}{r_r + sL_r\sigma} \tag{3.50}$$

A cascaded PI controller can be tuned for the appropriate speed of response for this system (Figure 3.5). The reference rotor speed is determined through the novel strategy developed in this work and described in the forthcoming manuscript.

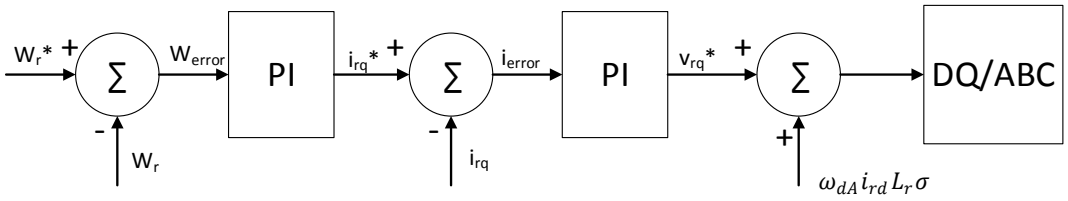

Figure 3.5: Speed control loop which takes a reference rotor speed as an input. The output of the block is the ABC phase voltages to be applied to the rotor.

3.1.3 Determination of Reference Speed

Described in manuscript.

4 Adjustable Speed Controls to Improve Efficiency and Flexibility of Set-Point Hydropower

Abstract-- Recent opportunities for new hydropower generation in the United States have often been in non-powered dams and run-of-river type flows occurring in low-impact natural areas and unregulated conduits. At the same time, a changing water resource paradigm is challenging some existing generation in drought stricken areas where supply reservoirs behind many medium and high head units are at historically low levels. The result is a developing market space which is potentially best captured by machines capable of variable speed operation. Variable speed units have a wider range of operating conditions compared to their synchronous counterparts and have already proven their resilience through a 20+ year history in pumped hydro applications. This work develops a control scheme for variable speed hydropower units operating to deliver a set-point power through flow controlling gates. This control scheme increases both the hydrologic operating range of a unit as well as the speed of response to grid contingencies under droop and automatic generator control. Results from simulation are confirmed on hardware.

4.1 Introduction

The history of hydropower in the United States is a story of reliability at an immense scale. Nearly 2,200 power stations built throughout the last 100 years combine to provide 80 GW of generating capacity – 7% of the national total - while also balancing the often competing priorities of flood risk management, irrigation, navigation, fisheries and wildlife management, and recreation. Almost half of this capacity is held in a relative handful of large (100-500MW) and very large (>500 MW) scale units located in the Columbia River basin of the Pacific Northwest. The hydroelectric system of that region in particular has served as a primary source of both traditional baseload and flexible power and has been a key enabler of the strong regional growth observed in nondispatchable wind and solar generation.

As is the case for the majority of large and very large hydropower plants in the US, the

power stations in the Columbia watershed have had and continue to need rehabilitation and modernization. This need, along with operational changes due to regulations, climate change, and a reprioritization of water use has led to decreasing capacity and availability factors throughout the US over the last several decades.

In addition to operational limitations, hydropower in some regions is also reaching its technical and economic ability to coordinate with and provide reserve to nondispatchable resources. Extraordinary ramping needs in conjunction with occasional negative market pricing due to the tax credits associated with wind and solar power add an additional challenge for operators managing hydropower plants which often have very little impoundment relative to their yearly stream flows and have obligations to release water throughout the year for purposes other than electric power production (*e.g.*. fish migration or flood risk management).

Hydropower developments which could enhance system flexibility in light of changing operating conditions and water resource paradigms could help secure the value proposition of hydropower and continue to support the growth of other renewable resources. Adding to that, the U.S. Department of Energy has set a goal of significantly increasing hydropower capacity through 2030 and increased flexibility to operate efficiently through a range of hydrologic conditions could create new opportunities for hydroelectric generation.

Developing the traditional synchronous speed hydropower generation paradigm into an adjustable speed system could help hydropower to increase flexibility, improve power system stability, and increase system efficiency at all scales. Previous work in this area has led to variable speed control systems designed to serve isolated loads through adjustable speed run of river systems [1], [2] or pumped hydropower coupled to wind generators [3]. Other studies have focused exclusively on control schemes for pumped storage in grid connected systems [4], [5]. Additionally, a significant amount of research has focused on variable speed control for axial flow systems without gates where speed is the only flow

regulator [6], [7] or where gates are in place but not available for governor control [8]–[11], sometimes explicitly because of constraints on maintaining a constant forebay elevation [12]. Underlying all of this work, physical testing has shown that variable speed operation can lead to extraordinary efficiency improvements for Kaplan turbines operating below nominal head [13] and an application of variable speed systems to an effluent stream has already achieved a successful outcome [14].

The variable speed control strategy developed in this work is an augmented governor which can quickly respond to grid contingencies, avoid exclusion zones, and arrive at the most efficient steady state operating point for a given set-point power through simultaneous control of gate position and turbine speed. This approach is applicable to small or large scale systems. Results on a variable speed hardware test bed confirm power capture improvement through adjustable speed control.

4.2 Variable Speed Operation

4.2.1 Hill Diagram

A prototype hydropower turbine is often characterized experimentally by varying flow and effective head in a laboratory to produce what is known as a Hill diagram or Hill chart (Figure 4.1) [15], [16]. The axes of the diagram are typically defined as the dimensionless flow rate and dimensionless speed of rotation,

$$Q_{ed} = \frac{Q}{D^2\sqrt{gH}} \tag{4.1}$$

$$N_{ed} = \frac{nD}{\sqrt{gH}} \tag{4.2}$$

where Q is the flow rate ($\frac{m^3}{s}$), D is the runner diameter (m), n is the rotational speed ($\frac{1}{s}$), H is the effective head (m), and g is the acceleration due to gravity ($\frac{m}{s^2}$) .

The utility of the Hill chart has historically been in evaluating the efficiency of a given

fixed speed system at high and low head scenarios through H. As will be shown, it is also possible to use the Hill to evaluate a system across multiple operating speeds through n in (4.2).

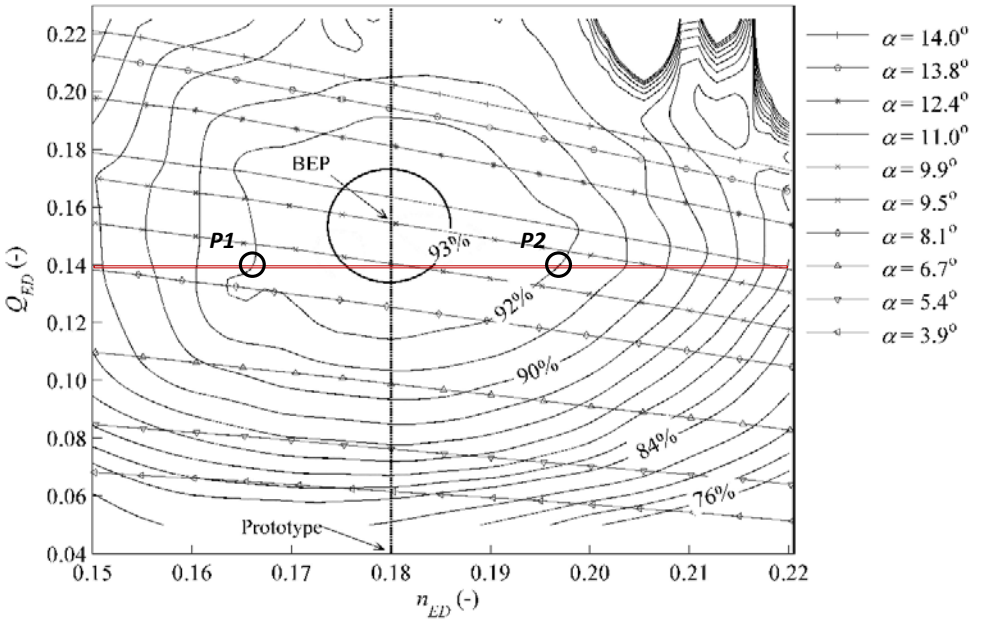

Figure 4.1: Hill diagram created by [17] through experimental testing of a Francis turbine. The dimensionless speed factor is shown along the abscissa and the dimensionless discharge factor is shown along the ordinate. The labels $P1$ and $P2$ are described in Subsection 4.2.3 and represent two operating points which deliver the same power at different speeds.

4.2.2 Mathematical approach to delivering set-point power in Adjustable Speed System

A key difference between fixed and adjustable speed systems is that fixed speed units have just one operating point where a specific set-point power can be delivered at a given available head. Gate position is the only control variable and efficiency cannot be optimized. Comparatively, adjustable speed operation introduces speed as an additional degree of freedom and enables a broader range of operating points for any given power and head combination. This can be seen mathematically by beginning with the equation for power in steady state,

$$P = \gamma Q H \eta \tag{4.3}$$

where γ is the specific weight of water ($\frac{N}{m^3}$) and η is efficiency.

This expression can be re-written through algebraic substitution of (4.1) with (4.3) as

$$P = \gamma\left(Q_{ed} * D^2\sqrt{H}\right)H\eta \tag{4.4}$$

Noting that large scale hydropower units are operated to deliver a specific set-point power at a known head, (4.4) can be rewritten with constants grouped to one side as

$$\frac{P}{\gamma D^2\sqrt{H} * H} = Q_{ed} * \eta \tag{4.5}$$

In combination with a Hill diagram, the implication of this expression is that there exists at least one $Q_{ed} * \eta$ operating point which satisfies the equality in (4.5)(4.5) for a given set-point *P* and known H. Back calculating through (4.2) to find the speed, *n*, for the (Q_{ed}, N_{ed}) pair associated with each satisfactory operating point reflects the flexibility of an adjustable speed unit and can be used by the augmented governor to maximize efficiency, avoid exclusion zones, *etc.*

4.2.3 Physical Justification through Euler's Pump and Turbine Equation

To confirm that the same power can be delivered at several different operating points, consider the line corresponding to $Q_{ed} = 0.14$ in the example Hill (Figure 4.1). Following the contours for efficiency it can be noted that there are two separate (Q_{ed}, N_{ed}) pairs, $P1$ and $P2$, which give the same $Q_{ed} * \eta$ product and therefore the same mechanical power per (4.5). Further, the actual flow, Q, is the same at each of the two operating points because Q_{ed} is constant. The only difference between the two operating points is the speed, n in N_{ed}, and the guide vane angle, α. The speed at $P2$ is higher and therefore the guide vane angle is larger to maintain the same flow.

The physical justification for each operating point making equivalent power in this example and for this system as a whole is seen through Euler's Pump and Turbine equation for turbo-machinery,

$$P = T\omega \tag{4.6}$$

$$T = \rho Q\left(C_{t,in}r_{in} - C_{t,out}r_{out}\right) \tag{4.7}$$

where $C_{t,in}$ and $C_{t,out}$ are the tangential velocities at the turbine inlet (outer edge of runner) and outlet (at the draft tube), respectively. Only tangential velocities contribute to the torque, T, on the turbine runner.

At $P1$ and $P2$ in the example Hill of Figure 4.1, all values in (4.7) are the same except $C_{t,in}$ and $C_{t,out}$. Per (4.6), both points can make the same power only if the torque at $P2$ is smaller because $P2$ is operating at a faster speed as is shown through (4.2).

The physical manifestation demonstrating that the torque at $P2$ will be lower can be confirmed through the velocity vectors shown in Figure 4.2.

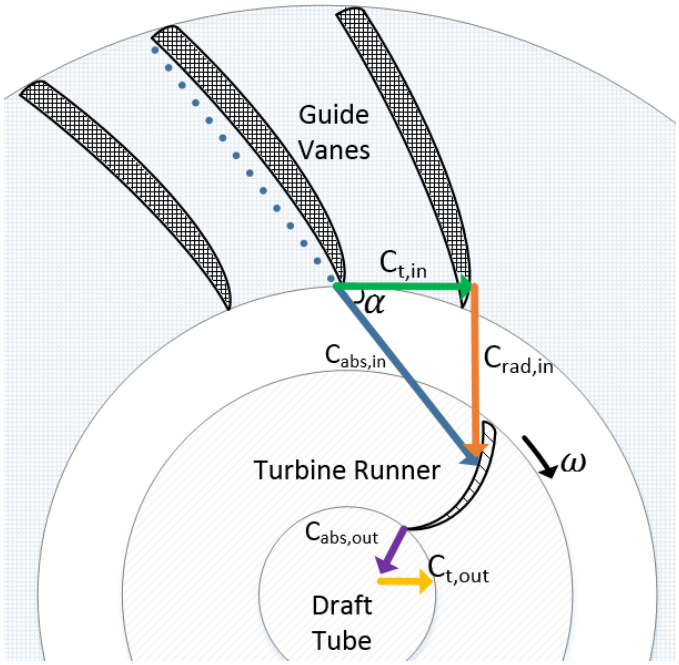

Figure 4.2: Top down axial view of a hydropower turbine showing water flowing through the guide vanes to act on the turbine runner before exiting down the draft tube. The absolute velocity of the incoming water, $C_{abs,in}$ (blue), can be separated into a tangential component, $C_{t,in} = C_{abs,in}\cos(\propto)$ (green), and a radial component, $C_{rad,in} = C_{abs,in}\sin(\propto)$ (orange). Only the tangential component contributes to the power producing torque. The larger guide vane angle, $\propto$, at P2 cf. P1 in Figure 4.1 is required to maintain constant flow at higher speed. The result is a smaller $C_{t,in}$ at P2 given the same $C_{abs,in}$ at both points.

In this diagram,

- $C_{t,in}$: The guide vane angle α is larger at $P2$ *cf.* $P1$ in order to maintain the same flow at higher speed. This results in a larger $\propto$ and therefore a smaller $C_{t,in}$ and, thus, a smaller torque at $P2$.
- $C_{t,out}$: Flow at the runner outlet co-rotates with the runner somewhat which results in the vector $C_{t,out}$ being positive near the best efficiency point (BEP). Noting that the flow is equal at both points, the velocity triangle at $P2$ will yield a larger $C_{t,out}$ and thus a smaller torque. Importantly, $C_{t,out}$ does not change proportionally with

$C_{t,in}$. Instead, $C_{t,out}$ is a function of runner rotational speed and flow rate through the turbine alone and is not dependent on guide vane angle.

These observations confirm that the power at $P1$ and $P2$ are the same because the torque at $P2$ is reduced due to the larger guide vane angle (which produces a smaller $C_{t,in}$) and faster speed (which produces a larger $C_{t,out}$). In a practical system, the choice between $P1$ and $P2$ could be made based on nearness to exclusion zones, synchronous speed, BEP, *etc*.; a lower speed or smaller guide vane angle would not necessarily be favored.

4.3 Governor Development & Machine Controls

The benefit of an adjustable speed hydropower system can be captured through an augmented governor which can control both the gate position and mechanical speed of the rotating system simultaneously. The combined augmented governor developed in this work is shown in Figure 4.3 and described in the forthcoming subsections. Importantly, $speed$ in this figure refers to the actual mechanical speed of the hydropower unit and $\Delta\omega$ refers to the deviation of grid frequency away from nominal per

$$\Delta\omega = (actual\ grid\ frequency - 1)\ p.u. \tag{4.8}$$

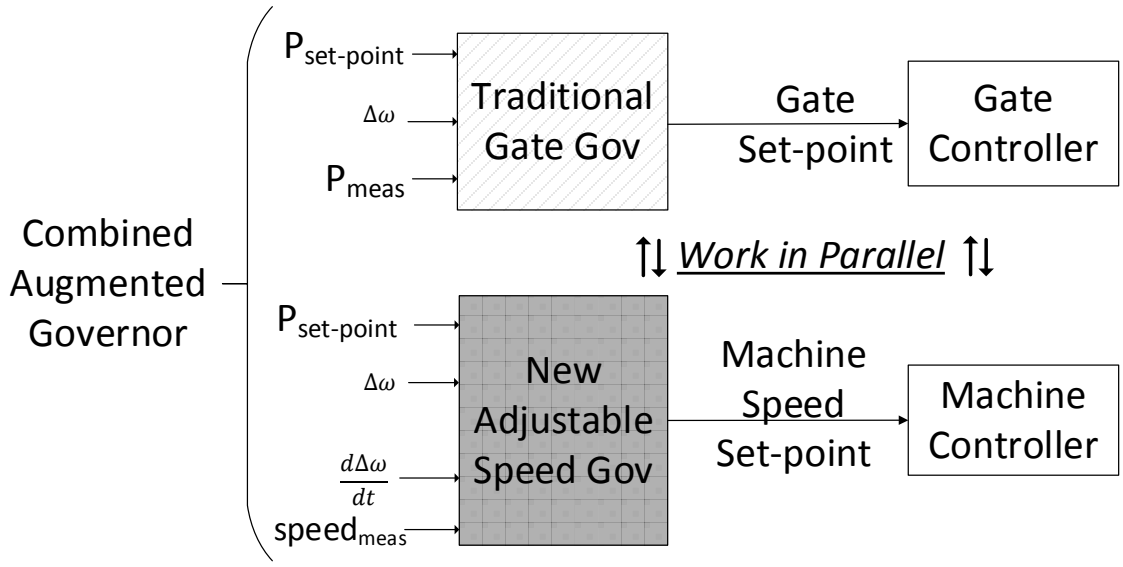

Figure 4.3: The new adjustable speed governor developed in this work operates in parallel with a traditional gate control governor. The traditional governor controls the gate (i.e. guide vane) position and the new adjustable speed governor controls the mechanical speed of the runner through the generator. The machine speed is quickly adjusted during transient to improve the speed of response and is then slowly re-adjusted in steady state to arrive at the most efficient operating point. Efficient operation uses less water to produce power.

4.3.1 Traditional Gate Control Governor

A traditional hydropower governor configured for load control (also commonly called speed regulation) uses a PID controller to open or close the guide vanes to deliver a set-point power (Figure 4.4). A watt meter at the output of the stator is used to feedback the power being generated in closed loop.

In addition to delivering an externally provided set-point power, the traditional governor also responds to grid frequency excursions, $\Delta\omega$, through a droop characteristic which automatically and autonomously changes the guide vane position on the order of seconds to tens of seconds to deliver more or less power as appropriate.

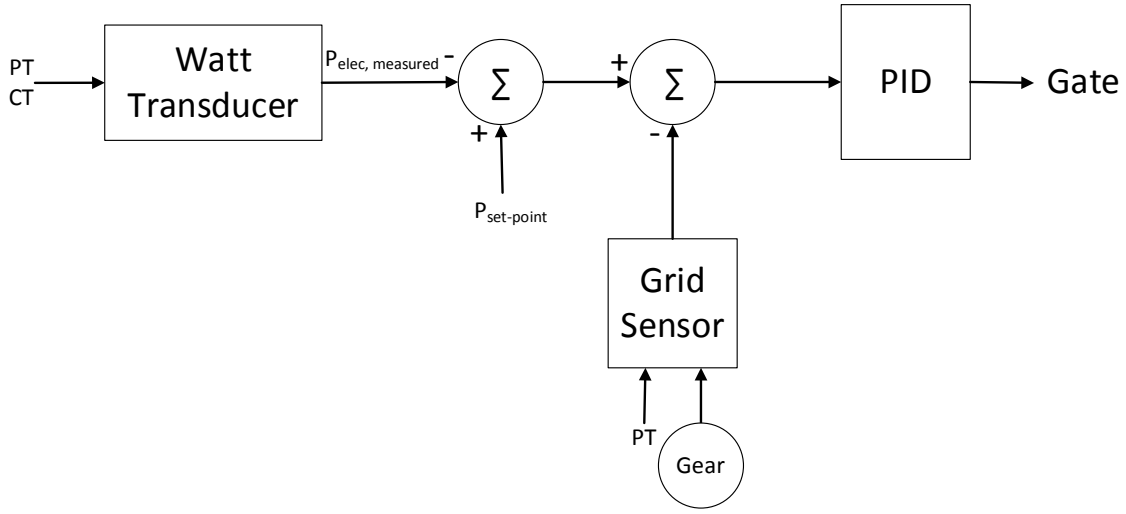

Figure 4.4: Traditional governor of a hydropower system operating under load control. A watt transducer at the output of the generator provides measured power as closed loop feedback to deliver a specified set-point power through the control variable of gate position. A larger gate position results in more flow and thus more power. This strategy of gate control is very well developed and is incorporated to a large portion of digital governors.

4.3.2 New Adjustable Speed Governor

The new adjustable speed governor uses a two stage strategy to improve the speed of response to grid contingencies in transient and to arrive at a steady state operating point which is optimized on the basis of efficiency or some other metric (Figure 4.5).

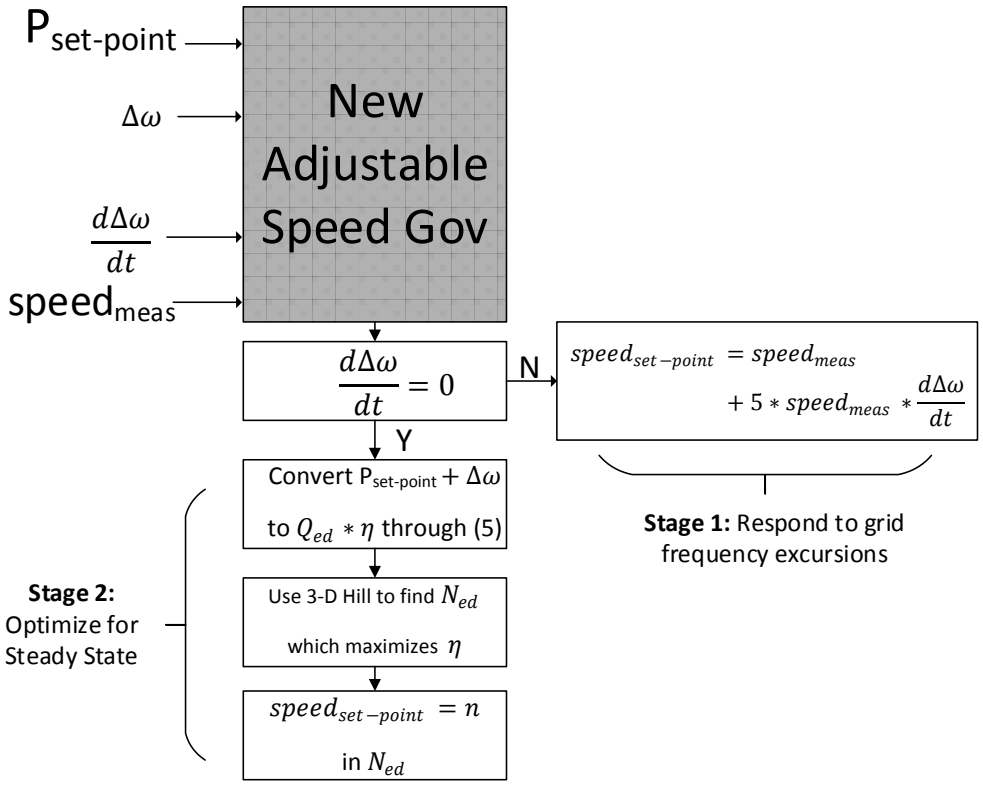

Figure 4.5: Process diagram of new adjustable speed governor developed in this work. The first stage responds to grid frequency excursions by changing machine speed in proportion to $\frac{\mathrm{d}\Delta\omega}{\mathrm{dt}}$. The second stage optimizes the machine speed to deliver the combined reference set-point power $\mathrm{P_{set-point}} + \Delta\omega$ in steady state.

The first stage responds to transient frequency excursions by changing the mechanical speed, $speed$, of the combined turbine and generator system by up to several percent in proportion to the rate of change of grid frequency, $\frac{\Delta\omega}{dt}$. In a falling frequency scenario, the system would be slowed to inject active power created through regenerative breaking. This initial response would result in a brief grid stabilizing spike in active power followed by a lower steady state output due to decreased efficiency at the new speed.

The second stage of control returns the system to the optimal steady state speed and gate position to deliver the set-point power with maximum efficiency. A change in machine speed which improves system efficiency will increase power production. The traditional

governor operating in parallel with closed loop feedback will automatically respond by closing the gates to maintain the set-point power.

The most efficient speed to deliver a given set-point power can be obtained by creating a 3D surface of a Hill diagram as shown in Figure 4.6. Recalling that $Q_{ed} * \eta$ is equivalent to power per (4.5), the most efficient operating speed, n in N_{ed} can be found as the maximum peak of the 3D surface along the line of constant power in $Q_{ed} * \eta$.

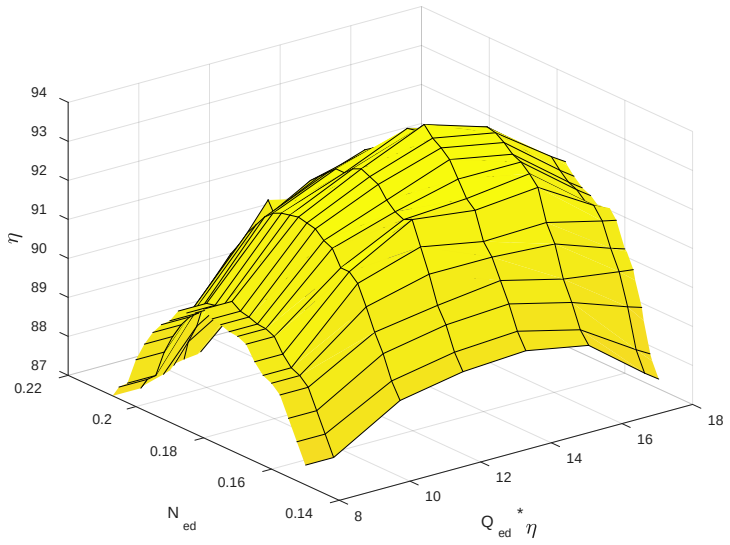

Figure 4.6: Hill diagram as a 3-dimensional surface. The BEP for a given set-point power is the speed in N_{ed} associated with the peak point for a given $Q_{ed} * \eta$ contor. Exclusion zones can be directly incorporated as boundaries to the surface.

4.4 Experimental Results

An advantage of the strategy developed in this work is that the adjustable speed governor finds an optimal speed set-point using a characterization of the turbine alone. This set-point value can then be provided as a speed reference to the machine controller for any type of electric generator connected in the hydropower system.

To demonstrate this flexibility, the augmented governor was tested in simulation using a model of a doubly-fed wound rotor induction generator (DFIG) and on hardware using a dynamometer physically connected to an induction machine operating as a generator through a variable frequency drive (VFD).

The transient scenario evaluated through experimentation is consistent between the simulation and hardware testing. A grid connected hydropower unit is operating in steady state to deliver a set-point power $P_{set-point} = 0.60\, p.u.$ to a nominal grid. A frequency excursion begins at time $t = 200\, sec$ with a slope $\frac{d\Delta\omega}{dt} = -0.00125\, p.u./sec.$ This is simulated to last for 2 seconds before being stabilized. The steady state frequency is then $0.9975\, p.u.$ which results in a continuous grid frequency deviation $\Delta\omega = -0.0025$ per (4.8).

The traditional governor of the hydropower system is equipped with a 5% droop characteristic and will therefore increase the generator output to deliver a new set-point power of $0.65\, p.u.$ on the basis of the combined input of $P_{set-point} + \Delta\omega$ provided to the traditional governor as previously shown in Figure 4.3 and Figure 4.4. The grid frequency excursion and corresponding impact on the combined reference set-point power through droop response is shown in Figure 4.7.

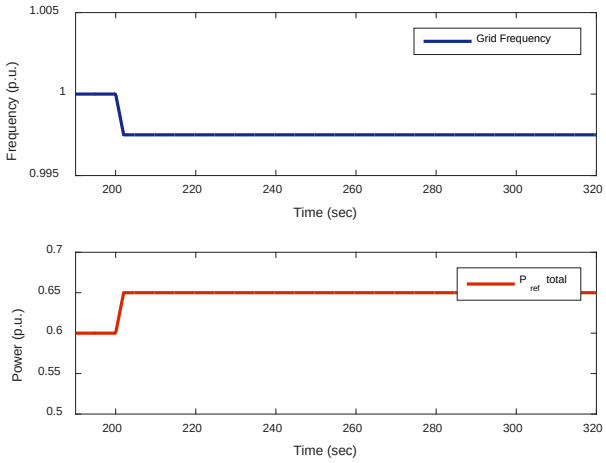

Figure 4.7: A grid frequency excursion occurs at *200* sec. This results in an increased combined reference signal through $P_{set-point} + \Delta\omega$.

The adjustable speed governor works in parallel with the traditional gate control system to enhance the primary frequency response to the transient by immediately slowing the machine at a rate of $5 * \frac{d\Delta\omega}{dt}\ p.u.$. After the transient is stabilized the adjustable speed governor slowly returns the system to the speed which maximizes efficiency for the new steady state combined input.

Using the 3-D Hill diagram of Figure 4.6 and assuming $Q_{ed} * \eta = 17.65$ represents a power of $1.0\ p.u.$ for the given system and can be considered as the base value in per unit calculations (*i.e.* $(Q_{ed} * \eta)_{base} = 17.65$), then per (4.5) the initial set-point value of $0.60\ p.u.$ corresponds to $Q_{ed} * \eta = (Q_{ed} * \eta)_{base} * 0.60 = 10.59$ and the final set-point value resulting from the combined input of the set-point and continuous deviation corresponds to $Q_{ed} * \eta = (Q_{ed} * \eta)_{base} * 0.65 = 11.4725$. Using the 3-D Hill, the most efficient operating speed for both states corresponds to the prototype speed of $N_{ed} = 0.18$. This is shown as $\omega = 1.0\ p.u.$ in the results subsections.

4.4.1 Simulation results

The overall system for simulation is shown in Figure 4.8. The adjustable speed governor provides a machine set-point speed as a reference to the DFIG speed controller connected to a 1.5 MW generator. The DFIG controller executes the speed through AC (super- and sub-synchronous) and DC (synchronous) excitation of the rotor circuit. A model is used to calculate the mechanical power of the turbine runner at a given gate position and speed. This power produces the generating torque on the DFIG.

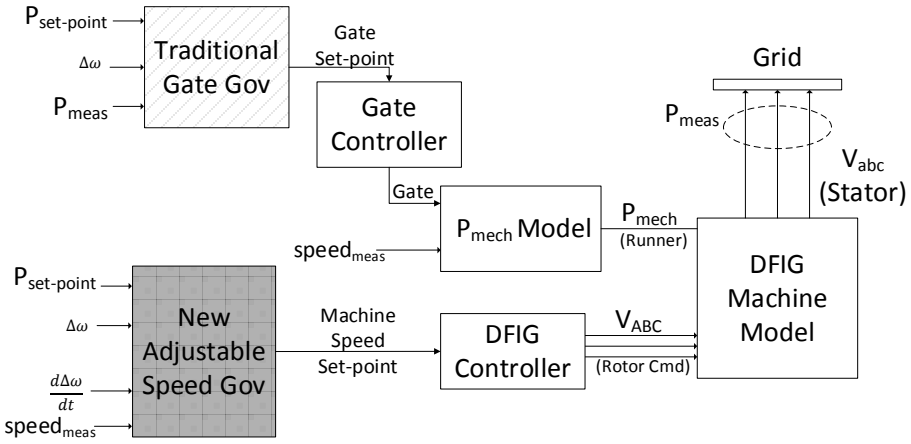

Figure 4.8: Complete block diagram of model used in simulation. The traditional and adjustable speed governors operate in parallel as an augmented combined governor. The DFIG controller executes the set-point reference from the adjustable speed governor. A model of the runner is used to calculate the mechanical power which produces the generating torque on the DFIG.

The model of the DFIG was developed according to [18]. Speed control to achieve a given reference was implemented using a cascaded PI controller as presented in [19]. The loop bandwidths and phase margins were tuned to match reference [20].

Results from simulation are shown in Figures 4.9-4.13. As can be seen, the rotor is rapidly slowed to a slip speed of ~5% (Figure 4.9) through the application of an AC rotor voltage (Figure 4.10). This results in an initial injection of active power as mechanical energy is converted into electrical energy through braking (Figure 4.11). The active power after

losses is as shown in Figure 4.12. When the grid transient is stabilized the rotor speed is momentarily held constant which results in a lower steady state power due to the decreased efficiency at the new, lower speed. The traditional governor continues to open the gates to work towards the set-point power and, after a brief period, the rotor speed is re-optimized (Figure 4.13).

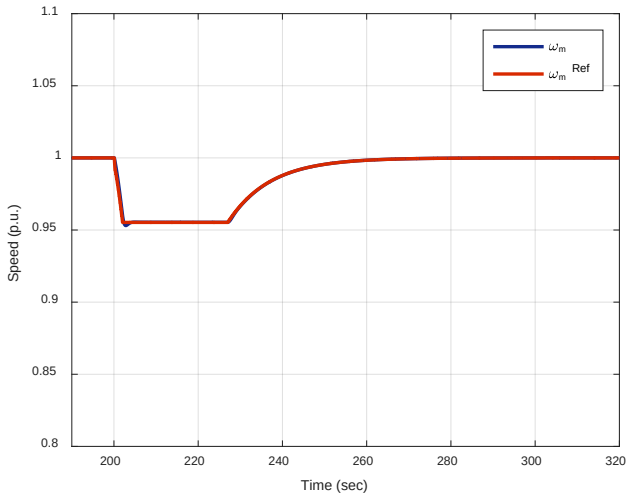

Figure 4.9: The adjustable speed governor detects the grid contingency and provides a reference speed to the DFIG speed controller to slow the rotor to inject active power. The rate of change of rotor speed is proportional to the rate of change of grid frequency.

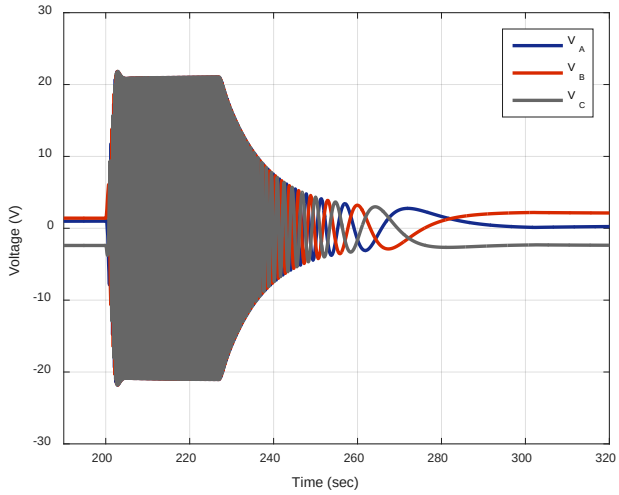

Figure 4.10: The DFIG speed controller applies sinusoidal excitation to the rotor circuit to achieve the sub-synchronous speed reference provided by the adjustable speed governor.

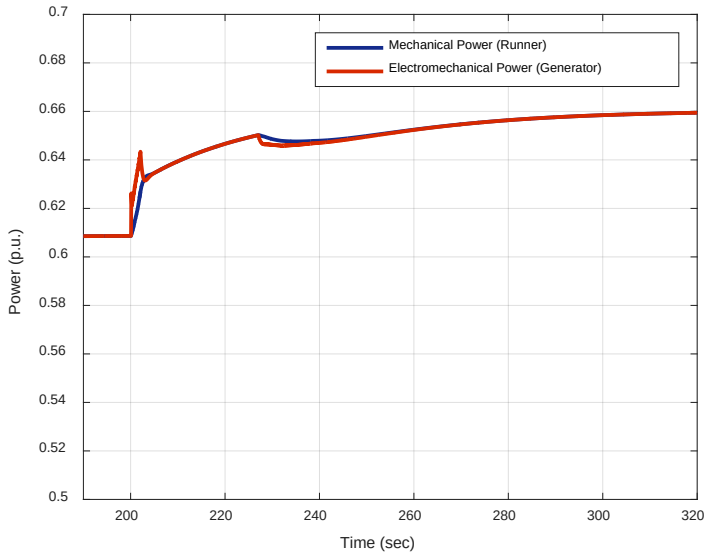

Figure 4.11: Comparison of the mechanical power of the runner which drives the generator vs. the electromechanical power produced by the DFIG. The braking torque applied at 200 seconds to slow the machine results in an injection of active power which can help halt a grid frequency excursion.

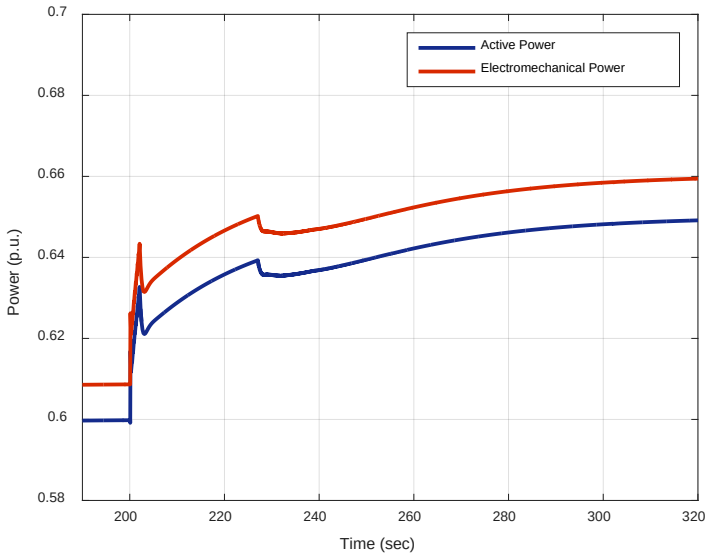

Figure 4.12: The electromechanical power is converted into active power which is measured at the point of grid connection to provide closed loop feedback to the augmented governor.

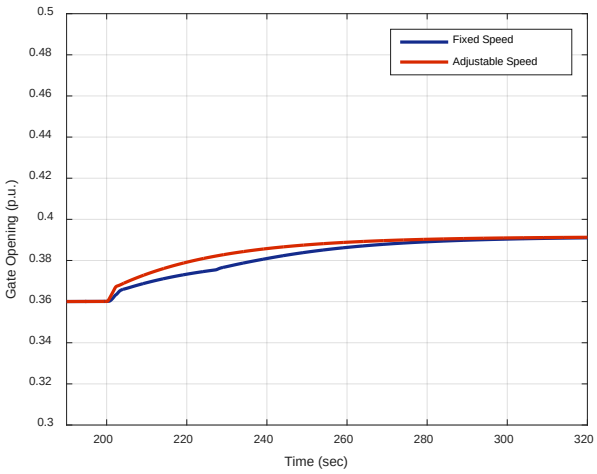

Figure 4.13: The traditional governor operates in parallel to control the gate position to achieve a set-point power through closed loop feedback. A comparison of the gate position over time from a system with and without adjustable speed operation shows that the sub-synchronous speed reference from the transient response results in a less efficient operating point and requires a larger gate opening to achieve the set-point power. The gate positions become equivalent as time passes on the account of the adjustable speed governor re-optimizing speed for steady state operation after the contingency has stabilized.

4.4.2 Hardware results

The augmented governor was tested on hardware through the configuration shown in Figure 4.14 and Figure 4.15. An induction generator is mechanically coupled to a 300 hp dynamometer operating under torque control. The dynamometer is driven to act as the turbine runner in a hydroelectric system using the model from simulation. A 20 kW ABB ACS-800 VFD connected to the stator terminals of the generator provides variable speed control using a reference from the adjustable speed governor.

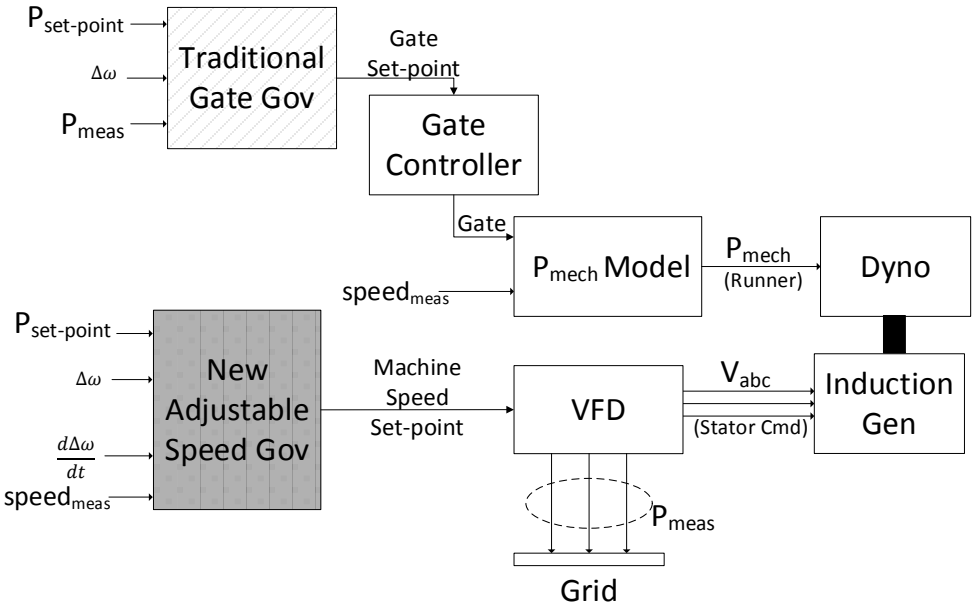

Figure 4.14: Laboratory configuration for hardware testing of the adjustable speed controller. A 300 hp dynamometer is driven in torque mode to represent the mechanical power of the turbine runner connected via rigid shaft to the generator. The generator is connected to the grid through a VFD at the stator terminals. Speed reference is provided to the VFD from the adjustable speed governor running through controlDesk.

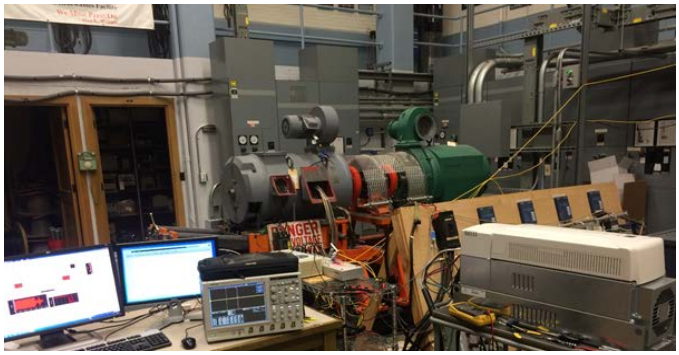

Figure 4.15: Picture of actual laboratory hardware. The 300 hp dyno (green, right) is physically connected to the induction machine (grey, left) which is driven through a 20 kW VFD (white and silver, bottom right). The execution and data logging of the hardware testing is managed through a PC running controlDesk (bottom left).

Results from hardware testing confirm that the adjustable speed governor can effectively work in parallel with a gate controller to increase the speed of response to grid contingencies and optimize efficiency. The speed reference from the adjustable speed governor was followed very closely by the VFD (Figure 4.16) and resulted in a large injection of active power which would enhance the primary frequency response of the generator (Figure 4.17). The magnitude of this response was such that the gate closed slightly in response to the increased measured power before continuing to open to deliver the new set point (Figure 4.18).

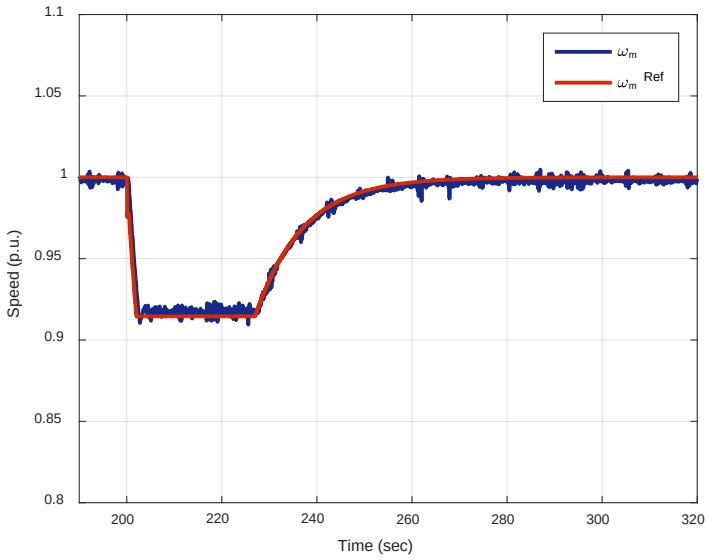

Figure 4.16: The adjustable speed governor provided a speed reference to the grid connected VFD which enabled variable speed operation of the induction generator under test. A small 0.015 p.u. offset was applied to correct for DAC drift.

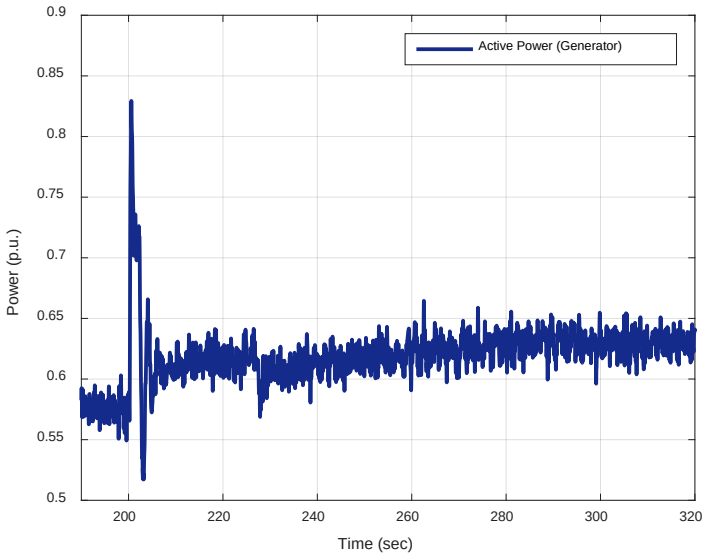

Figure 4.17: Slowing the machine in response to the grid contingency resulted in a large spike in active power injection which enhances the primary frequency response of the generating unit. Power continues to increase after the transient on the account of the gate opening and the speed being re-optimized for efficiency.

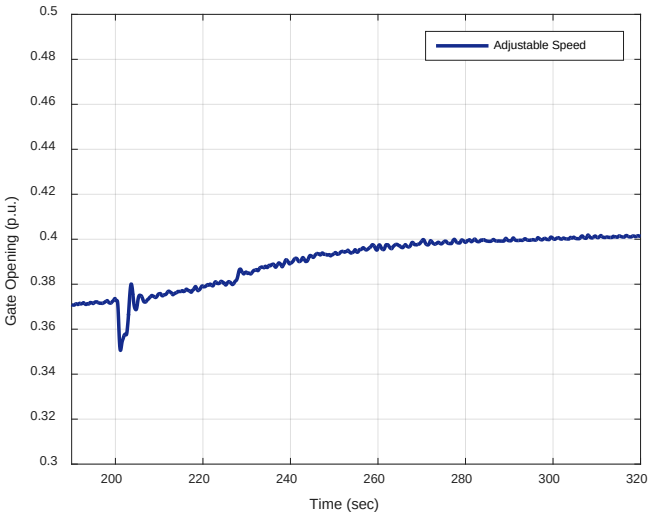

Figure 4.18: The gate opening increased after the contingency to deliver the new combined set-point reference of the original set-point power plus the new continuous deviation from nominal grid frequency. The magnitude and duration of the active power injection from variable speed operation at the time of the transient was such that the gates closed slightly initially before re-opening to continue towards the new set-point.

4.5 Conclusions and Future Work

The adjustable speed governor developed in this work shows promise as a tool to increase the flexibility of hydropower generators by broadening the efficient operating range and improving the speed of response to grid contingencies.

The first stage of the two stage governor was shown to increase active power injection in response to grid frequency excursions. This enhances the primary frequency response of hydropower units through adjustable speed operation.

The second stage of the adjustable speed governor was shown to optimize the unit speed to the most efficient operating point for a given combined reference set-point power. This

was accomplished through a 3-dimensional Hill with axes of power, speed, and efficiency. Exclusion zones can be directly implemented on the 3-D surface.

Future work will develop enhanced physical models of the turbine under variable speed control in order to tune the traditional and adjustable speed governors in the context of physical effects due to changing water speeds.

Additionally, the ACS-800 is capable of four-quadrant operation and could be connected directly to the rotor windings of a DFIG for hardware validation of the simulation described in this work.

4.6 References

[1] M. U. Akhtar, “Variable speed drive as an alternative solution for a micro-hydro power plant,” 2012.

[2] A. Ansel and B. Robyns, “Modelling and simulation of an autonomous variable speed micro hydropower station,” vol. 71, pp. 320–332, 2006.

[3] J. A. Suul, “Variable speed pumped storage hydropower plants for integration of wind power in isolated power systems,” 2009.

[4] D. Schafer, “Adjustable speed Asynchronous Machine in Hydro Power Plants and its Advantages for the Electric Grid Stability.”

[5] O. Nagura, M. Higuchi, K. Tani, and T. Oyake, “Hitachi’s adjustable-speed pumped-storage system contributing to prevention of global warming,” *Hitachi Rev.*, vol. 59, no. 3, pp. 99–105, 2010.

[6] J. Fraile-Ardanuy, J. R. Wilhelmi, J. J. Fraile-Mora, and J. I. Pérez, “Variable-speed hydro generation: Operational aspects and control,” *IEEE Trans. Energy Convers.*, vol. 21, no. 2, pp. 569–574, 2006.

[7] J. Wilhelmi and J. Fraile-Ardanuy, “Adjustable speed hydro generation,” *Proc. Int. …*, 2003.

[8] J. I. Pérez-Díaz and J. Fraile-Ardanuy, “Neural networks for optimal operation of a run-of-river adjustable speed hydro power plant with axial-flow propeller turbine,” *2008 Mediterr. Conf. Control Autom. - Conf. Proceedings, MED’08*, pp. 309–314, 2008.

[9] K. F.-M. Fraile-Ardanuy, Jesús, J. I. Perez, I. Sarasua, J.R. Wilhelmi, “Speed Optimisation Module of a Hydraulic Francis turbine based on Artificial Neural Networks. Application to the Dynamic Analysis and Control of an Adjustable Speed Hydro Plant,” no. 1, pp. 4104–4110, 2006.

[10] M. P. M. A. A. Borghetti, M. Di Silvestro, G. Naldi, “Maximum Efficiency Point Tracking for Adjustable-Speed Small Hydro Power Plant,” *16th PSCC*, pp. 1–7, 2008.

[11] J. Fraile-Ardanuy and J. Wilhelmi, “A dynamic model of adjustable speed hydro plants,” *Proc. 9 Congr. …*, 2005.

[12] J. R. Wilhelmi, J. I. Pérez, and I. Sarasúa, “Speed control of run-of-river variable speed hydro plants,” *Int. Conf. Renew. Energy Power Qual.*, 2006.

[13] G. P. Heckelsmueller, “Application of variable speed operation on Francis turbines,” *Ing. e Investig.*, vol. 35, no. 1, pp. 12–16, 2015.

[14] N. Y. S. E. R. and D. Authority, “Hydropower from Wastewater,” no. 12, 2011.

[15] G. Olimstad, T. Nielsen, and B. Børresen, “Stability Limits of Reversible-Pump Turbines in Turbine Mode of Operation and Measurements of Unstable Characteristics,” *J. Fluids Eng.*, vol. 134, no. 11, p. 111202, 2012.

[16] G. a. Aggidis and A. Zidonis, “Hydro turbine prototype testing and generation of performance curves: Fully automated approach,” *Renew. Energy*, vol. 71, pp. 433–441, 2014.

[17] N. at NTNU, “First Workshop (2014) - Experimental Study.” [Online]. Available: https://www.ntnu.edu/nvks/experimental-study.

[18] N. Mohan, *Advanced Electric Drives: Analysis, Control, and Modeling Using MATLAB/Simulink*. John Wiley & Sons, 2014.

[19] P. Pourbeik, “Grid Integration and Dynamic Impact of Wind Energy [Book Reviews],” *Power Energy Mag. IEEE*, vol. 11, no. 2, pp. 91–92, 2013.

[20] T. K. A. Brekken, “A novel control scheme for a doubly-fed induction wind generator under unbalanced grid voltage conditions,” *Oregon State Univ. Corvallis*, 2005.

5 Conclusions and Future Work

The goal of this research was to develop and test an adjustable speed control scheme for hydropower systems operating under set-point power control. The motivation for this effort was the potential to enhance the operational flexibility and efficiency of hydroelectric generators by adding speed as a new degree of freedom.

The approach taken in this work was to first understand the water resource, policy, and economic landscape in which a potential variable speed system would be operating. The reason for this initial step was to identify constraints and potential emerging applications which could create new operational regimes and benefit designs accessible only through adjustable speed operation. The outcome of that analysis showed that adjustable speed operation could enhance grid stability and broaden the efficient operating range of hydropower generators at all scale.

A novel control scheme was then developed, simulated, and tested on hardware. This underlying basis of this new strategy was a physics-based understanding of pump and turbine hydraulics. Data from an experimentally characterized turbine was used to create a 3-dimensional surface of efficiency and an adjustable speed governor was developed to draw a reference speed from the surface to maximize efficiency for a given set-point power. This governor worked in parallel with a traditional governor for gate control and was shown to increase the magnitude and speed of response to grid frequency extrusions. This effect was observed both in simulation on a model of a DFIG and on hardware using an induction generator connected to the grid through a VFD.

Future work can develop an independent, physics based model for a turbine operating under adjustable speed control. This model will enable the adjustable speed governor to be tuned in the context of non-linear hydraulic effects associated with speed changes which may not have been captured in the presented work.

Using the enhanced model, additional future work can execute hardware testing on an electric generator connected to a turbine system operating in the field to confirm performance improvement and identify opportunities for further enhancement.

6 Bibliography

[1] U. S. D. of Energy, “2014 Hydropower Market Report,” 2015.

[2] U. S. D. of Energy, “2014 National Hydropower Map,” 2014. [Online]. Available: http://nhaap.ornl.gov/content/national-hydropower-map. [Accessed: 01-Jan-2016].

[3] U. S. E. I. Administration, “The Columbia River Basin provides more than 40% of total U.S. hydroelectric generation.” [Online]. Available: No Titlehttp://www.eia.gov/todayinenergy/detail.cfm?id=16891. [Accessed: 20-Jun-2005].

[4] N. RiverPartners, “Northwest Hydropower and Columbia Basin River Benefits,” 2013.

[5] N. P. and C. Council, “A guide to major hydropower dams of the columbia river basin,” 2013. [Online]. Available: https://www.nwcouncil.org/energy/powersupply/dam-guide. [Accessed: 01-May-2016].

[6] U.S. Army Corps of Engineers, U.S. Bureau of Reclamation, and Bonneville Power Administration, “Federal Columbia River Power System,” no. August, 2003.

[7] B. P. Administration, “Power benefits of the lower Snake River dams,” 2009.

[8] Bonneville Power Administration, “Major Dams Within Columbia River Basin.”

[9] B. P. Administration, “Wind Generation & Total Load in The BPA Balancing Authority,” 2014.

[10] U. S. D. of Energy, “Hydropower Projects Fiscal Years 2008 - 2014,” 2014.

[11] H. R. Foundation, “BLUE GOLD : Building New Hydropower With Existing Infrastructure,” 2015.

[12] US Army Corps of Engineers, “Outlook for the U.S. Army Corps of Engineers Hydropower Program,” 2011.

[13] U. S. D. of Energy, *An assessment of energy potential at non-powered dams in the United States*, no. April. 2012.

[14] *16 U.S.C. 791a-825r*. .

[15] B. P. ADMINISTRATION, U. S. B. O. RECLAMATION, and U. S. A. C. O. ENGINEERS, “The Columbia River System Inside Story,” p. 80, 2001.

[16] K. Brettmann, “Managing Skagit River Basin Dams for Flood Risk Management,” 2016.

[17] Bonneville Power Administration, “Columbia River Basin Fish Restoration Activities: Acomplishments to Date and Upcoming Issues,” 2015.

[18] C. Raymond, “2015 IN THE CONTEXT OF CLIMATE CHANGE: IMPLICATIONS FOR MANAGEMENT,” 2016.

[19] U. S. E. I. Administration, “Annual Energy Outlook 2015,” 2015.

[20] U. S. E. I. Administration, “Electricity Data Browser.” [Online]. Available: http://www.eia.gov/electricity/data/browser/#/topic/0?agg=2,0,1&fuel=vvg&geo=g&sec=g&freq=M&datecode=null&rtype=s&start=200101&end=201602&ctype=linechart&ltype=pin&pin=&rse=0&maptype=0&linechart=ELEC.GEN.ALL-. [Accessed: 01-May-2016].

[21] U. S. E. I. Administration, “Demand trends, prices, and policies drive recent electric generation capacity additions,” 2016. [Online]. Available: http://www.eia.gov/todayinenergy/detail.cfm?id=25432. [Accessed: 01-May-2015].

[22] Caiso, “What the Duck Curve Tells Us About Managing a Green Grid,” pp. 1–4, 2013.

[23] U. S. E. I. Administration, “Solar, natural gas, wind make up most 2016 generation additions.” [Online]. Available: http://www.eia.gov/todayinenergy/detail.cfm?id=25172. [Accessed: 01-May-2016].

[24] M. U. Akhtar, “Variable speed drive as an alternative solution for a micro-hydro power plant,” 2012.

[25] A. Ansel and B. Robyns, “Modelling and simulation of an autonomous variable speed micro hydropower station,” vol. 71, pp. 320–332, 2006.

[26] J. A. Suul, “Variable speed pumped storage hydropower plants for integration of wind power in isolated power systems,” 2009.

[27] D. Schafer, “Adjustable speed Asynchronous Machine in Hydro Power Plants and its Advantages for the Electric Grid Stability.”

[28] O. Nagura, M. Higuchi, K. Tani, and T. Oyake, “Hitachi’s adjustable-speed pumped-storage system contributing to prevention of global warming,” *Hitachi Rev.*, vol. 59, no. 3, pp. 99–105, 2010.

[29] J. Fraile-Ardanuy, J. R. Wilhelmi, J. J. Fraile-Mora, and J. I. Pérez, “Variable-speed hydro generation: Operational aspects and control,” *IEEE Trans. Energy Convers.*, vol. 21, no. 2, pp. 569–574, 2006.

[30] J. Wilhelmi and J. Fraile-Ardanuy, “Adjustable speed hydro generation,” *Proc. Int. …*, 2003.

[31] J. I. Pérez-Díaz and J. Fraile-Ardanuy, “Neural networks for optimal operation of a run-of-river adjustable speed hydro power plant with axial-flow propeller turbine,” *2008 Mediterr. Conf. Control Autom. - Conf. Proceedings, MED’08*, pp. 309–314, 2008.

[32] K. F.-M. Fraile-Ardanuy, Jesús, J. I. Perez, I. Sarasua, J.R. Wilhelmi, “Speed Optimisation Module of a Hydraulic Francis turbine based on Artificial Neural Networks. Application to the Dynamic Analysis and

Control of an Adjustable Speed Hydro Plant," no. 1, pp. 4104–4110, 2006.

[33] M. P. M. A. A. Borghetti, M. Di Silvestro, G. Naldi, "Maximum Efficiency Point Tracking for Adjustable-Speed Small Hydro Power Plant," *16th PSCC*, pp. 1–7, 2008.

[34] J. Fraile-Ardanuy and J. Wilhelmi, "A dynamic model of adjustable speed hydro plants," *Proc. 9 Congr. …*, 2005.

[35] J. R. Wilhelmi, J. I. Pérez, and I. Sarasúa, "Speed control of run-of-river variable speed hydro plants," *Int. Conf. Renew. Energy Power Qual.*, 2006.

[36] G. P. Heckelsmueller, "Application of variable speed operation on Francis turbines," *Ing. e Investig.*, vol. 35, no. 1, pp. 12–16, 2015.

[37] N. Y. S. E. R. and D. Authority, "Hydropower from Wastewater," no. 12, 2011.

[38] G. Peter and J. Day, "2009 BPA facts," pp. 5–6, 2011.

[39] Bonneville Power Administration, "BPA transmission : moving the power of the Northwest."

[40] E. W. and E. Board, "EWEB 's Slice and Block Contract with BPA," pp. 1–2, 2011.

[41] E. W. and E. Board, "Electric Resources Portfolio," 2012. [Online]. Available: http://www.eweb.org/resources/portfolio. [Accessed: 01-May-2016].

[42] E. Hiaasen, "BPA Post 2011 Contract Amendments and Tier 2 Election," 2014.

[43] E. Water and E. Board, "Annual Report on Power Trading Compliance and Financial Results," pp. 1–5, 2015.

[44] Bonneville Power Administration, “2012 BPA Final Rate Proposal: Power Loads and Resources Study,” vol. BP-12-FS-B, no. July, p. 54, 2011.

[45] PacificCorp, “2015 IRP Update,” *J. Chem. Inf. Model.*, vol. 53, no. 9, pp. 1689–1699, 2013.

[46] U. S. E. I. Administration, “Negative prices in wholesale electricity markets indicate supply inflexibilities,” 2012. [Online]. Available: https://www.eia.gov/todayinenergy/detail.cfm?id=5110. [Accessed: 01-May-2016].

[47] Nerc, “Balancing and frequency control,” p. 53, 2011.

[48] E. Ela, M. Milligan, and B. Kirby, “Operating Reserves and Variable Generation,” *Contract*, no. August, pp. 1–103, 2011.

[49] B. J. Kirby, *Frequency Regulation Basics and Trends*, no. December. 2004.

[50] J. M. Bert, “Ancillary services : Technical and Commercial Insights,” *Orthop. Clin. North Am.*, vol. 39, no. 1, pp. 1–4, v, 2008.

[51] NERC, “Ancillary Services Matrix,” *Ferc*, pp. 1–19.

[52] Bonneville Power Administration, “BP-14 Generation Inputs Workshop,” 2012.

[53] J. D. Wellschlager, “National Wildlife Federation vs. National Marine Fisheries Services and United States Army Corps of Engineers.”

[54] Merriam-Webster, “cross section of a hydroelectric power plant.” [Online]. Available: http://www.visualdictionaryonline.com/energy/hydroelectricity/hydroelectric-complex/cross-section-hydroelectric-power-plant.php#generator-unit6979. [Accessed: 01-May-2016].

[55] U. S. A. C. of Engineers, “Electrical Generator.”

[56] E. Britannica, “Francis vs Kaplan.” [Online]. Available: http://kids.britannica.com/comptons/art-53475/Turbines-are-used-to-convert-the-energy-in-a-stream. [Accessed: 01-May-2016].

[57] I. P. S. D. P. Committee, I. P. S. S. Subcommittee, and I. T. F. on T.-G. Modeling, “PES-TR1: Dynamic Models for Turbine-Governors in Power System Studies,” 2013.

[58] K. Astrom, “Productivity Improvements in Assembly,” 2014.

[59] “Voith Hydro.” .

[60] T. Bechtel and M. E. Fabbri, “Enhancement of Hydroturbine Operational Flexibility for Powerplant Cost Optimization,” 2014.

[61] N. Mohan, *Advanced Electric Drives: Analysis, Control, and Modeling Using MATLAB/Simulink*. John Wiley & Sons, 2014.

[62] P. Pourbeik, “Grid Integration and Dynamic Impact of Wind Energy [Book Reviews],” *Power Energy Mag. IEEE*, vol. 11, no. 2, pp. 91–92, 2013.